Development of functional biobased microencapsulation systems for textile applications

Guilherme Andreoli Gil

Final dissertation submitted to **Escola Superior de Tecnologia e Gestão** of **Instituto Politécnico de Bragança** to obtain the Master's Degree in **Chemical Engineering** in the ambit of the double diploma with the **Universidade Tecnológica Federal do Paraná - Câmpus Apucarana**

Supervisors

Prof. Doctor Maria Filomena Barreiro

Prof. Doctor Caroline Casagrande Sipoli

Doctor Isabel Patrícia Fernandes

Bragança

2020

To my family, for education, love and encouragement at all times of my life.

“Everyone has inside of him a piece of good news. The good news is that you don’t know how great you can be! How much you can love! What you can accomplish! And what your potential is!”

(Anne Frank)

ACKNOWLEDGEMENTS

To my supervisors, Prof. Dra. Maria Filomena Barreiro and Dra. Isabel Patrícia Fernandes, from IPB, and Prof. Dr. Caroline Casagrande Sipoli, from UTFPR, excellent people and professionals, who guided me with their vast knowledge, my deep thanks for empathy, availability, attention, motivation and support for this work to become a reality.

To the Universidade Tecnológica Federal do Paraná for welcoming me and being my home during my undergraduate years. To the Instituto Politécnico de Bragança for the receptivity during the double diploma program. To each of the professors, servants and employees who contribute to the aggrandizement of these institutions and the realization of our dreams.

To all teachers, from my basic education to graduation, who with great mastery taught me the art of knowledge and the guidelines of life. In particular, to my undergraduate supervisors, Prof. Dr. Murilo Pereira Moisés and Prof. Dr. Fabricio Maestá Bezerra, all my gratitude for the trust, friendship and opportunities that opened so many doors for me. To Prof. Dr. Manuel Lis Arias, from UPC-Terrassa, for sharing all his knowledge at such an important time in my life. And to the Golden Technology company, for trusting my work in the more than 3 years of project developed in partnership with UTFPR. All of you have been fundamental in my personal, professional and cultural growth throughout my undergraduate studies.

To my parents, Júnior Cesar and Maria Angélica, who have supported me throughout my life and have never gone to any lengths to make my dreams come true. To my brothers, Renan and Matheus, for their friendship and companionship. To my aunt, Rosa Maria, who since my childhood has played a key role in my personal and academic growth. To my grandmother, Luiza, who with her gift of teacher and wisdom, taught me from an early age the importance of study and the love of books. To my late grandfather, Cristobal, who will always be my inspiration of character and honesty.

To my girlfriend, Nayra, who made me believe in the realization of this dream. I will be forever grateful for your support, love, complicity, companionship and for encouraging me from the beginning to complete this journey. I also leave all my gratitude to your parents, Nivaldo and Elaine, for the friendship, affection and encouragement.

To all my friendships, which were present at different times in my life. Thank you for turning moments into laughter and joy. I will be forever grateful to each one of you, who today I don’t mention in names, but in spirit, for the great moments lived from my childhood to the present day.

This work was partially funded by the Portuguese Foundation for Science and Technology (FCT, Portugal) and FEDER under the PT2020 program - financial support to CIMO (UIDB / 00690/2020).

ABSTRACT

Essential oils have been widely used in the textile sector due to their numerous properties and health benefits. Terpenes are the main components of essential oils being limonene one of the most abundant one in nature. Microencapsulation systems based on natural products have emerged as an important tool for the preservation and controlled release of essential oils. In this context, the present work was devoted to the increase of scale of a previously studied microencapsulation process of limonene by complex coacervation method. Chitosan (CH) and gum Arabic (GA) were used as shell materials and (R)-(+)-limonene as the core material. The complex coacervation is based on the formation of a colloidal system in which oppositely charged biopolymers complex and coat oil droplets. After this initial step, the formed microcapsules are hardened through crosslinking of chitosan with tannic acid. The study was divided in the following three different sections: (i) optimization of the process variables and analysis of their influence on the microcapsule's morphology, where the influence of the homogenization stage (emulsion formation), stirring rate, geometry of the stirring impeller, volume and concentration of tannic acid solution, emulsifier type and the final washing step, was studied leading to an optimized and reproducible process; (ii) study of the biopolymers concentration and oil amount effect on process productivity; and (iii) characterization of the microcapsules produced in the last assays. The microcapsules obtained by inserting 4 mL of tannic acid solution 10% (w/v) showed spherical morphology. The reactor stirring using an impeller with two plane and vertical blades at 150 rpm promoted efficient fluid dynamic flow and thermal exchange. The emulsifier PGPR 4125 (polyglycerol polyricinoleate) was chosen due to its non-toxicity and biodegradability, guaranteeing the stability of the emulsion and uniform dispersion of the oil droplets. The analysis by optical microscopy proved the effectiveness of inserting a final washing step to remove unreacted raw materials. The analysis of the solids content revealed a possible excess of the shell materials or dragging of the microcapsules in the washing step, due to the low values attained, even when the limonene amount was increased. In all assays, microcapsules with perfectly spherical morphologies were identified. The microcapsules had a small mean particle size, between 1.92 and 2.42 μm, which is in accordance with the size range given in the literature (1 to 500 μm) for microcapsules produced by the complex coacervation method. A high encapsulation efficiency was attained, ranging from 99.2% to 99.7%. From the overall analysis of the performed study, it can be considered that the production

of limonene CH-GA microcapsules using a laboratorial scale reactor (capacity 1L) was successfully achieved. Thus, the production of limonene microcapsules by the complex coacervation method, using natural raw materials offer the possibility to be scalable, increasing their potential application in the textile industry.

Keywords: Textile Sector; Microencapsulation, Natural Products; Complex Coacervation; Process Optimization.

RESUMO

Os óleos essenciais têm sido amplamente utilizados no setor têxtil devido às suas inúmeras propriedades e benefícios para a saúde. Os terpenos são os principais componentes dos óleos essenciais, sendo o limoneno um dos mais abundantes na natureza. Os sistemas de microencapsulação à base de produtos naturais têm surgido como uma importante ferramenta para a preservação e liberação controlada de óleos essenciais. Nesse contexto, o presente trabalho foi dedicado ao aumento de escala de um processo previamente desenvolvido envolvendo a microencapsulação de limoneno pelo método de coacervação complexa usando um reator de bancada encamisado equipado com um sistema de controlo de temperatura e um agitador mecânico. O quitosano (CH) e a goma arábica (GA) foram utilizados como materiais de cápsula e o (R)-(+)-limoneno como material de núcleo. O método de coacervação complexa é baseado na formação de um sistema coloidal no qual biopolímeros de carga oposta complexam revestindo gotas de óleo. Após esta etapa inicial, as microcápsulas formadas são endurecidas por meio da reticulação do quitosano com ácido tânico. O estudo foi dividido em três seções: (i) otimização das variáveis do processo e análise da sua influência na morfologia da microcápsula, onde a influência do estágio de homogeneização (formação da emulsão), velocidade de agitação, geometria do agitador, volume e concentração da solução de ácido tânico, tipo de emulsificante e a etapa final de lavagem, foram estudados levando a um processo otimizado e reprodutível; (ii) estudo do efeito da concentração de biopolímeros e da quantidade de óleo na produtividade do processo; e (iii) caracterização das microcápsulas produzidas nos últimos ensaios. No que respeita às condições testadas, as microcápsulas obtidas quando se adicionou 4 mL de solução de ácido tânico a 10% (m/v) apresentaram morfologia esférica. A agitação do reator utilizando uma pá do tipo impulsor com duas lâminas planas e verticais a uma velocidade de 150 rpm promoveu eficiente fluxo fluido dinâmico e troca de calor. O emulsificante PGPR 4125 (poliricinoleato de poliglicerol) foi escolhido devido à sua atoxicidade e biodegradabilidade, garantindo a estabilidade da emulsão e uma boa dispersão das gotas de óleo. As análises de microscopia ótica comprovaram a eficácia da inserção de uma etapa de lavagem final para remover as matérias-primas que não reagiram. A análise do teor de sólidos revelou valores baixos, podendo estes serem atribuídos a um possível excesso de materiais encapsulantes, que são removidos nas etapas de lavagem juntamente com algumas das microcápsulas de menor dimensão. Em todos os ensaios, foram

identificadas microcápsulas com morfologias perfeitamente esféricas. As microcápsulas apresentaram um tamanho médio de partícula entre 1,92 e 2,42 μm, que está de acordo com o intervalo de tamanho dado na literatura (1 a 500 μm) para microcápsulas produzidas pelo método de coacervação complexa. A eficiência de encapsulação manteve-se elevada, estando os valores obtidos entre 99,2% a 99,7%. De uma perspectiva geral, pode considerar-se que a produção de microcápsulas de limoneno usando um reator à escala laboratorial (capacidade 1L) foi alcançada com sucesso. Assim, a produção de microcápsulas de limoneno pelo método de coacervação complexa, utilizando matérias-primas naturais, pode apresentar viabilidade de aumento de escala, indicando o seu potencial de aplicação na indústria têxtil.

Palavras chave: Setor Têxtil; Microencapsulação; Produtos Naturais; Coacervação Complexa; Otimização do Processo.

LIST OF CONTENTS

INDEX OF FIGURES

INDEX OF TABLES

Appendix

GLOSSARY

ATR-FT-IR – Fourier-transformed Infrared Spectroscopy Attenuated Total Reflection

BTCA – 1,2,3,4-butane-tetracarboxylic Acid

CCO – Complex Coacervation

CH – Chitosan

CM – Confocal Microscopy

DLS – Dynamic Light Scattering

EE – Encapsulation Efficiency

EO – Essential Oil

FDA – Food and Drug Administration

FT-IR – Fourier-transformed Infrared Spectroscopy

GA – Gum Arabic

GC – Gas Chromatography

GC-FID – Gas Chromatography with Flame Ionization Detector

GRAS – Substance Generally Recognized as Safe

HLB – Hydrophilic-lipophilic Balance

MS – Mass Spectroscopy

MW – Molecular Mass

NASA – National Aeronautics and Space Administration

OM – Optical Microscopy

PC – Polyelectrolytic Complexes

PGPR – Polyglycerol Polyricinoleate

SCO – Simple Coacervation

SEM – Scanning Electron Microscopy

TA – Tannic Acid

TGA – Thermogravimetric Analyzes

UK – United Kingdom

US – United States

UV – Ultraviolet

1 INTRODUCTION

1.1 Motivations and Objectives

The textile sector corresponds to one of the most active, competitive and important sectors of the Portuguese economy, being responsible for 3% of the national Gross Domestic Product, due to the high generated employment and financial flux [1,2]. Currently, Portugal exports around 80% of the national textile production, which involves 189 countries, with Spain, France, Germany, United Kingdom, United States of America, Italy and the Netherlands, as the major markets. The commercial and economic success, and the rapid rise of the number and importance of the Portuguese textile companies are justified by the strong investment in technology, design and innovation [2].

The textile industry is in constant process of innovation, driven by scientific investments leading to the development of technologies and products capable of improving the performance of the textile substrates [3]. Moreover, in the last decade, textile industries in Western Europe, Japan and the United States of America have invested deeply in the microencapsulation market with the objective of developing functional and intelligent textiles with high added value, thus promoting comfort and interaction with the individual [4]. In this sense, products based on microencapsulation were developed to provide several properties, such as, treatment of muscle pain, anti-cellulite treatment, skin hydration, long-lasting of fragrances, and controlled release of drugs and antimicrobial agents [5,6].

Microencapsulation systems based on natural products occupy a prominent place in the market, in view of commercial differentiation, non-toxicity, and biodegradability conferred by natural and natural-derived polymers, and the health benefits provided by the encapsulated substances [7,8]. In recent years, interest in the use of essential oils as active agents has increased due to their antioxidant, antimicrobial and medicinal properties [9]. Essential oils are extracted from a wide variety of plants and herbs, having terpenes and terpenoids in their composition, which are responsible for the properties mentioned previously. However, essential oils are extremely sensitive to environmental conditions, depending on protection strategies to preserve their properties, and maintain their functionalities [10,11].

In brief, microencapsulation consists in the imprisonment of a substance, such as an essential oil, in extremely small particles (shell or matrix type) capable of protecting

it from harmful environmental conditions and/or conferring controlled release, which can be driven by physical or chemical stimuli [12,13]. In the present work, microcapsules will be produced based on a previous work of the group, where chitosan/gum Arabic particles with antimicrobial properties imparted by limonene were produced by coacervation [6,14,15]. Limonene, a terpene present in the most abundant essential oils in nature, will be used as the active principle in view of its pleasant aroma and antimicrobial properties in fabrics [16]. The main objectives were to settle the conditions to increase the scale production with reproducibility. Moreover, modifications to the former formulation have been studied in order to increase limonene load.

In this context, the present work will be developed according to the following sequential parts:

1. In the first part of the project, microcapsules were produced at an increased scale, namely 200 mL, in a jacketed batch reactor equipped with stirring and temperature control. Microcapsules of chitosan/gum Arabic will be produced by complex coacervation using the best formulations proposed in a previous work [15]. The use of the proposed batch reactor aims to better control the synthesis conditions assuring reproducibility and the later possibility of industrial application of the studied process.
2. A systematic study considering the factors influencing the synthesis conditions were carried out in order to analyze and improve the quality of the encapsulation system. In this part, visual analysis and optical microscopy were used to evaluate the morphological features of the microcapsules during the the assays. The process to variables to be studied are: volume and concentration of tannic acid; stirring rate; homogenization step; type of emulsifiers; type of stirring impeller; and influence of the final washing step.
3. The third part of the work is devoted to the study of the effect of biopolymers concentration and volume of essential oil, in order to evaluate their effect on the microcapsules productivity and impact on chemical and morphological properties of the microcapsules. The obtained microcapsules physical appearance will be evaluated by optical microscopy, being the solid content also determined.
4. The last section correspond to the characterization of the microcapsules produced in the final assays in terms of particle size. In addition, the encapsulation efficiency will be also determined in order to validate the strategies adopted having in view future developments of functional and intelligent textiles.

1.2 Layout

The dissertation was divided into five chapters. The first chapter correspond to the Introduction, where the study object is contextualized, followed by the description of the motivation and main objectives. *Chapter 2* encloses the literature review, made in order to provide a theoretical framework of the main topics of this study. Then, *Chapter 3* is dedicated to the materials and applied methods description. *Chapter 4* encloses the main results and discussion regarding the analysis of the process variables with influence on the physicochemical properties of the microcapsules and microencapsulation efficiency. Finally, *Chapter 5* corresponds to the main conclusions drawn from this work, enclosing also suggestions for future works.

2 LITERATURE REVIEW

2.1 Textile Industry and Innovation

Innovation in products and processes enables organizations to reach a prominent place in the international market and, consequently, to promote their economic growth [17]. Innovation gives rise to new forms of competition and cooperation, as well as to institution's uniqueness in their market segment [18]. In addition, many institutions focus on the development of green and sustainable technologies in the production and product's application [18].

Since 2004, the European textile industry has adopted a new strategy to re-establish its position in the international market. This strategy consists of developing new products from innovative technologies aiming at improving textile properties or design textiles with completely new properties [19]. Technologies such as oil and water repellency, stain repellency, UV protection, flame retardancy, self-cleaning, energy storage, antistatic properties, wrinkle resistance, antimicrobial properties, and controlled drug release add high value to the so-called unconventional textiles [19,20].

Nanotechnology is the most promising and sustainable technology in the world and the textile industry is one of its main customers. Currently there has been a strong growth in the production of smart, functional and high performance textiles through the application of nanomaterial's coatings and finishes [20]. The high demand for materials that exert some functionality to the textile substrate motivated the increase in research and the interest to develop new studies in this area.

2.2 Natural Origin Systems

Criticisms of the textile industry due to its harmful practices to the environment and consumer awareness have led companies to initiate a productive reformulation and seek for new environmentally less aggressive raw materials, services and products. In this sense, systems of natural origin have emerged as ecological alternatives, which are less toxic, and biodegradable thus attracting the attention of researchers and companies [8].

In recent years, natural products, such as plant essential oils and biopolymers (gelatins, alginates and polysaccharides), have been used as sustainable raw materials in the green synthesis of nanoparticles [8]. Hydrogels, emulsions, liposomes, microspheres

and microparticles based on natural products have resulted in products with potential application in several areas.

Therefore Moghimipour and coworkers prepared liposomes based on soy lecithin and cholesterol loaded with essential oil of *Eucalyptus camaldulensis* with the objective of improving the stability and solubility in water, besides guaranteeing its fungicidal efficacy against dermatophytes [21]. Sharkawy and coworkers developed vanillin and limonene microcapsules via green synthesis by complex coacervation using chitosan and gum Arabic as shell materials to promote antimicrobial effect and perfume release on cotton fabric [15]. In the study developed by Chan and coworkers, the encapsulation of an aqueous plant-based extract (*Piper sarmentosum)* with spheres of Ca-alginate hydrogel was used to evaluate the effect of process variables on the encapsulation efficiency and stability of biological compounds [22].

Summarizing, there is an enormous interest in the use of plant essential oils as the core material in encapsulation systems of natural origin. For this reason, the next topic will be dedicated to biopolymers and essential oils to deepen the knowledge about the chemical composition and properties that can guarantee its industrial application for the benefit of human health.

2.3 Biopolymers

2.3.1 Chitosan

Chitosan (CH) is a cationic polysaccharide of natural origin obtained from the deacetylation of chitin (N-acetyl-D-glucosamine). Chitin is a linear polymer, in fibrous state, present in the exoskeleton of insects and crustaceans [23,24]. Structurally, CH is composed of beta-(1-4) linked 2-acetamide-2-deoxy-D-glucose (A-unit) and 2-amino-2-deoxy-D-glucose (D-unit) [25]. The chemical structures of chitin and chitosan are shown in Figure 1.

The amine groups ($-NH_2$) present in the chemical structure of chitosan (with a degree of deacetylation greater than 50%) are predominantly positive at pH below 6.5 [25]. Thus, pH is an important tool when the objective is the electrostatic interaction of chitosan with anionic poly-anions (such as gum Arabic, carboxymethyl cellulose,

alginates, pectins, xanthan and gelatin) for complex formation [25,26]. In addition, its solubility in water is directly linked to the pH of the medium [25].

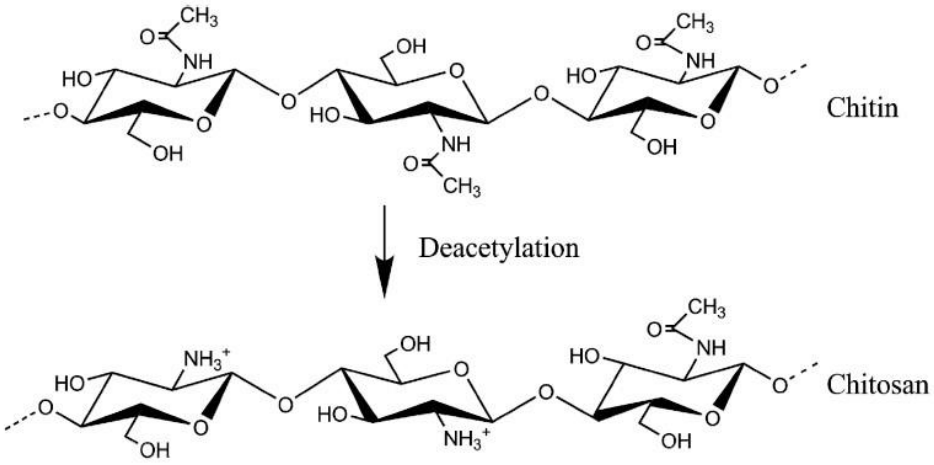

Figure 1 – Chemical structure of chitin and chitosan
Source: Adapted from Nilsen-Nygaard *et al.* [25].

The growing industrial interest in CH is mainly due to its biodegradability, biocompatibility, non-toxicity, solubility in aqueous medium, antimicrobial effect, and because it is extracted from an economically viable and abundant source in nature [24,26,27]. These characteristics make chitosan an advantageous alternative to other synthetic and natural polymers. For these reasons, companies in the agricultural, food, pharmaceutical, medical and textile sectors are strongly investing in studies involving chitosan, with the aim of developing innovative and ecological products [24].

2.3.2 Gum Arabic

Gum Arabic (GA) is an anionic polymer found in trees of *Acacia* species, such as *Acacia senegal* and *Acacia seyal*, the two most popular and main sources of commercial gum. *Acacia* trees are commonly found in semi-arid regions of sub-Saharan Africa, although species of this genus exist in different countries of the world [28]. GA is highly heterogeneous and consists of a gummy exudate from the sap expelled by the tree's stem and branches, which solidifies in contact with air [28,29].

GA is a complex branched polysaccharide composed mainly of arabin and a mixture of calcium, magnesium and potassium salts of Arabic acid. The chemical composition of the polysaccharide fraction basically contains galactose (39-42%),

arabinose (24-27%), rhamnose (12-16%), uronic acids (15-16%) and glyco-proteins (1,5-2.6%) [29,30]. However, the chemical composition is liable to change according to the species and age of the tree, location (climatic conditions and soil), in addition to the exudation time [29]. In Figure 2 the chemical structure of the branched chain of gum Arabic with the respective chemical groups is presented.

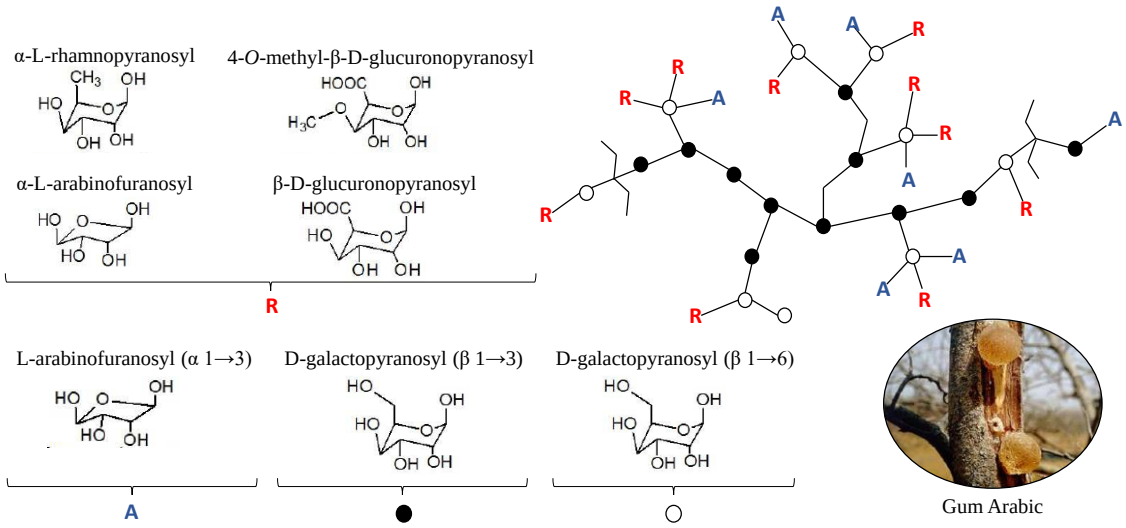

Figure 2 - Representation of the main groups that make up the complex chemical structure of gum arabic. Source: Adapted from Quintanilha [29].

Gum Arabic is a biodegradable and biocompatible polymer, being the main source of polysaccharides used in the formation of complex molecule carriers, due to its structural and functional properties [26,31]. At neutral pH their -OH groups dissociate resulting in a high level of negative charges that interact electronically with cationic polymers [26]. At acid pH, it has a potential emulsifying activity, since its hydroxyl groups increase the hydrophilicity of the medium [32,33]. GA also acts as a flocculant, stabilizer, thickening agent and food additive, in addition to have a nephroprotective, antioxidant, anti-inflammatory character, and being easily soluble in water (up to 48% w/v in cold water). All of these properties promoted the use of GA in the food, cosmetic, textile, ceramic, medical and pharmaceutical industries [28,30].

2.4 Essential Oils

Studies on the effects and industrial applicability of essential oils had strong progresses following the improvement of characterization techniques such as

chromatography, microscopy and spectroscopy analysis [9]. In the search for natural alternatives to replace synthetic products, the main applications of essential oils are focused on the pharmaceutical, cosmetic, food, textile, agricultural and perfumery industries due to their antimicrobial, antioxidant, medicinal, pharmacological, aromatic and esthetic properties [34–36].

Essential oils (EO) are a complex blend of highly volatile aromatic compounds, existent in a wide variety of plants and herbs. They are sensitive to heat and UV radiation and are easily oxidized [9,10,37]. The amount of essential oil varies from 1 to 8% of the total weight of the vegetable matrix [38]. The main components of essential oils are terpenes (monoterpenes and sesquiterpenes) and phenylpropanoids mixed with small molecules like alcohols, ketones, esters and aldehydes of short chain [11,37,39].

The antimicrobial effect of an EO is due to the presence of compounds such as carvacrol, thymol, cinnamaldehyde and eugenol [10]. In Table 1 a set of some essential oils found in the literature, focusing research in diverse areas, and their respective chemical compositions and properties are presented.

The chemical composition of EO depends on many factors, such as plant species, age, collected part, origin, climate, soil, use of agrochemicals, extraction method and storage time [39]. Currently, the chemical composition of essential oils is determined by Gas Chromatography (GC) coupled with Mass Spectroscopy (MS) [39].

Terpenes are the main components of EO and are the responsible for antimicrobial, antidiabetic, anticancer, antioxidant, antiallergic and anti-inflammatory activities. The terpene structure can be defined as formed by isoprene units (Figure 3).

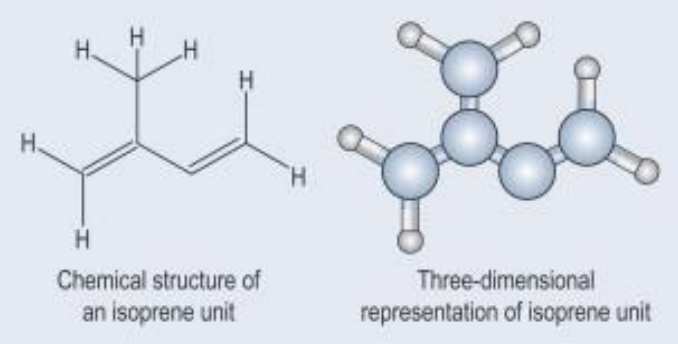

Figure 3 - Chemical structure of an isoprene unit.
Source: Adapted from Aldred [40].

Table 1 - Examples of essential oils with their respective chemical compositions and properties.

Oil	Chemicals Components	Properties	References
 **Oregano** *Origanum vulgare* Linnaeus	Carvacrol, thymol, ρ-cymene, ethyl caprate, myrcene, ledol, α-pinene, β-pinene, camphene, α-terpinene, γ-terpinene, cineole, linalool, ledol and β-bisabolene.	Antimicrobial, antifungal, antioxidant, antispastic and antiseptic effect. Flavoring and preservative in food products.	[41–43]
 **Rosemary** *Rosmarinus officinalis* Linnaeus	1,8-cineole, bornyl acetate, borneol, limonene, camphene, camphor, myrcene, α-terpineol, β-caryophyllene, α-pinene and β-pinene.	Antimicrobial, analgesic, anti-inflammatory, anti-ulcerogenic, antioxidant, circulatory stimulant and food preservative. Inhibit spoilage and pathogenic bacteria.	[39,41,44]
 **Citronella** *Cymbopogon nardus* Rendle* *Cymbopogon winterianus* Jowitt**	*Camphene, citronellol, geraniol, limonene and methyl isoeugenol. **Citronellol, citronellal, elemol, geraniol and geranyl acetate.	Biopesticide non-toxic, antidepressant, deodorant, antibacterial, anticonvulsant, anxiolytic, antipyretic, diuretic, sterilant and insect repellent.	[35,38,45]
 **Lavender** *Lavandula angustifolia* Miller	Linalool, 1,8-cineole, myrcene linalyl anthranilate, linalyl acetate, α-pinene, α-terpineol, borneol, camphor, carvone, lavandulyl acetate, geranyl acetate caryophyllene, eucalyptol and neryl acetate.	Antibacterial, antifungal, analgesic and anti-ulcerogenic. Relieves symptoms of anxiety, stress and depression (aromatherapy).	[46–48]
 **Sweet orange** *Citrus sinensis* L.	D-limonene, octanal, β-myrcene, α-pinene, β-linalool, cyclohexene and decanal.	Antibacterial, antioxidant, anti-cancer and insecticide activity.	[49–51]
 **Wild mint** *Mentha longifolia*	Sabinene, α-pipene, , β-pinene, , β-myrcene, limonene, 1,8-cineole, menthone, isopulegone, pulegone, carvone, piperitenone, piperitenone oxide, caryophyllene and germacrene D.	Antiparasitic, antibacterial, insecticide, antimutagenic, anti-inflammatory, antioxidant, antinociceptive, keratoprotective, hepatoprotective and spasmolytic	[52,53]

Among these limonene is one of the most abundant terpenes in nature and is widely used at industrial level due to the above mentioned properties, besides having a strong aroma and flavor [16]. On the other hand, its low water solubility and easy oxidation are challenges to be overcome in the design of effective applications [13].

The (R)-(+)-limonene is a cyclic monoterpene of molecular formula $C_{10}H_{16}$ (MW = 136.24 $g.mol^{-1}$), boiling point of 176 ºC, vapor pressure at 20 ºC of 213 Pa and a solubility in water at 25 ºC of 10.6 $mg.L^{-1}$ [54]. It is a renewable nonpolar solvent, colorless, and the main component of the oil extracted by cold pressing and distillation from the peels of citrus fruits, such as lemon and orange. Moreover, it can be obtained from the residue of some industries, being a relatively cheap raw material for use as a core material in encapsulation [55,56]. The chemical structure of limonene is shown in the Figure 4.

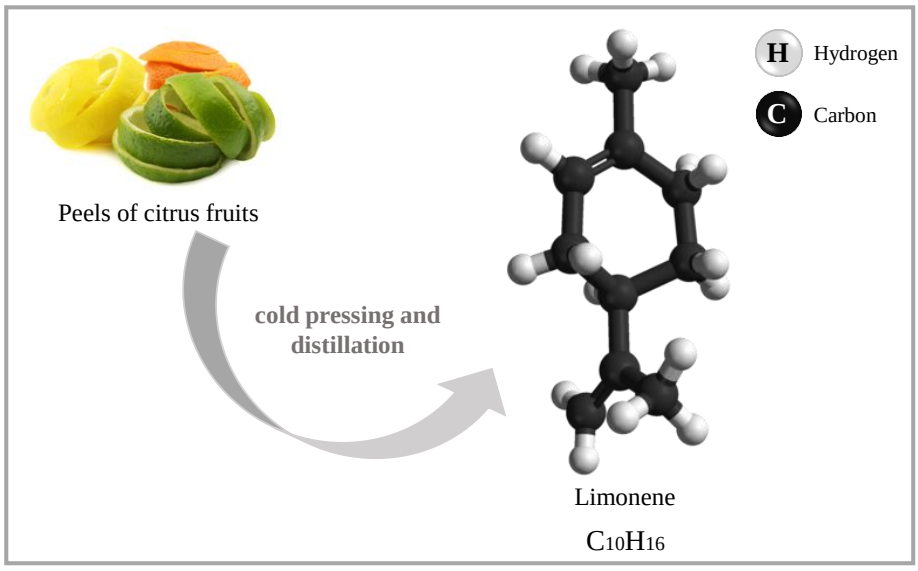

Figure 4 - Chemical structure of limonene.
Source: Adapted from World Of Chemicals [57].

The oil extraction can be done by steam distillation, hydrodistillation, solvent extraction, and supercritical fluid extraction using the complete vegetable or parts thereof (leaves, flowers, fruits, seeds, roots and bark) [38,58]. The obtained oil quality and process yield are directly dependent on biotic and abiotic factors such as plant genetics, light incidence, water availability and pest and predator attack, as well as the used type of extraction process [9].

Steam distillation is the most recommended technique for large scale production, but high process temperatures may cause degradation of thermolabile compounds [39]. Hydrodistillation is a simple, economically viable and cost-effective method for EO extraction. It enables the obtainment of a good quality product. Solvent extraction is a simple and economically viable method, but solvent traces in the oil can be harmful to the consumer. Supercritical fluid extraction gives rise to excellent quality oil obtained at high efficiency, but needing an initial high investment [38]. However, in recent years, due to the strong environmental appeal, green extraction has proved to be a prosperous extraction method. Green extraction is based on processes with reduced energy consumption, use of alternative solvents and renewable natural products, in addition to the obtainment of good quality oil [58].

Essential oils are composed by numerous lipophilic components, which are susceptible to degradation when exposed to environmental conditions [34]. In addition, characteristics such as high volatility, low stability, low water solubility, and remarkable aroma and taste, require the application of encapsulation procedures through liposome, emulsion or nanoparticulate systems [49,59]. Recently, encapsulation systems to protect EO, and other natural products, are being increasingly gaining importance in productive systems, and to reach innovative markets.

2.5 Microencapsulation and Techniques

The encapsulation strategy consists of trapping a substance in extremely small particles [60]. Microencapsulation is a technique of packing solid, liquid or gaseous materials through a continuous polymeric membrane to form small particles, called microcapsules or microspheres, which are designed to release their content in a controlled manner and predetermined conditions [37,61,62]. Therefore microencapsulation is the incorporation of an active principle molecule in an ordered polymeric structure [12]. Microencapsulation technologies are applied in different fields of study, such as pharmaceutical, textile, cosmetic, food and agricultural pesticides [63].

The main purpose of microencapsulation is to protect the core material from environmental stimuli and control the release of volatile active ingredients, besides increase its stability and availability over time [27,64]. Thus, it is possible to modify the properties of the active compounds and transform liquid substances into solid materials

in order to facilitate their handling and application [65]. Microencapsulation systems are very important to protect essential oils from chemical degradation and improve its water compatibility [13]. These, together with other purposes and benefits of oil microencapsulation, are shown in the Figure 5.

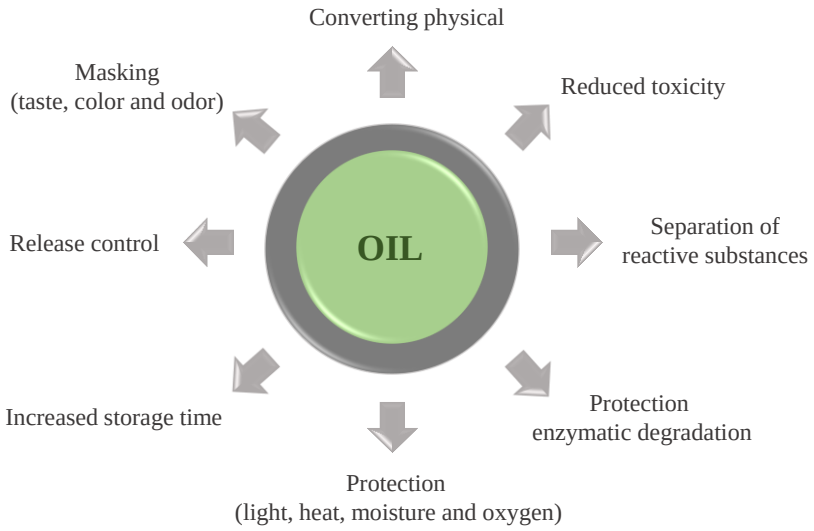

Figure 5 - Purposes and benefits of oil microencapsulation.
Source: Adapted from Martins *et al.* [6].

The microcapsules have a particle size in the range 0.2–5000 μm, and different morphologies according to the characteristics of the materials involved in their production [61]. The structural composition of a microcapsule is composed by an external layer of a polymeric material, called wall, coating, shell, or membrane, and a filler consisting of the an active agent, called internal phase or core material [66]. The combination of the wall material with the core material results in multi-core, multi-shell or simple microcapsules [67]. Multi-core microcapsules contain numerous droplets of the active principle molecules inside, while multi-shell microcapsules contain two or more layers of the polymeric material as shell. The simple morphology microcapsules contain only one active material molecule and one shell layer [67].

Microcapsules carrying oil as the active principle have different morphologies according to the synthesis technique and the crosslinking mechanism, as illustrated in Figure 6. According to the structural organization of the microcapsules they are classified as follows [6]:

- *Irregular shaped capsule*: Amorphous wall structure with distributed hydrophilic and hydrophobic compounds. Oil molecules interact with hydrophobic compounds forming several small oil cores within the shell material protection;
- *Polynuclear capsule*: Well-defined spherical wall with distributed hydrophilic and hydrophobic compounds throughout the material. Oil molecules interact with hydrophobic compounds forming several small oil cores with shell material protection. The disadvantages are the presence of cores near the walls facilitating oil loss and degradation, as well as low oil load capacity;
- *Oil core shell capsule*: Well-defined spherical wall with a single oil core in the center. Capacity to encapsulate large volume of oil and promote good stability;
- *Emulsion core shell capsule*: Well-defined spherical structure with the presence of a single core filled with an emulsion that allows the simultaneous encapsulation of hydrophilic and hydrophobic compounds.

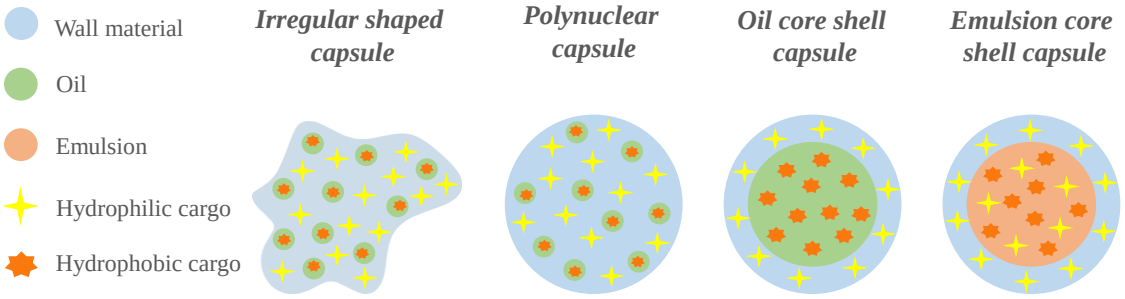

Figure 6 - Microcapsule structure with encapsulated oil.
Source: Adapted from Martins *et al.* [6].

The microcapsule shell material can be a polymer of natural, semi-synthetic or synthetic origin [68]. There are a wide variety of shell materials that are applied in microencapsulation processes, including synthetic polymers, co-polymers, carbohydrate polymers, cellulosic materials, starch derivatives, maltodextrins, gums, proteins and lipids [36,67,69]. Some properties are indispensable for the success of the coating material, such as provide the stabilization of the encapsulated substance, being inert towards the core material, ensure controlled release of the core material under specific

conditions, provide flexibility, stability, solubility in aqueous or solvent medium, present low viscosity, being non-hygroscopic and economically viable [70].

The core material is an active principle whose application provides some finishes and functionality to the microcapsules. The most commonly applied core materials are drugs, oils, essential oils, flavors, fragrances, repellents, colorants, vitamins, probiotics and cosmetic substances [68,69,71,72]. The physical state of the core material directly influences the microcapsule morphology. Generically, liquid core materials give rise to spherical microcapsules, while crystalline solids give rise to irregular microcapsules [67].

The microcapsule production techniques are classified according to the nature of the process involved in their synthesis, as shown in Table 2. There are three different classifications for microencapsulation processes [65]:

1. *Physical*: The polymers reacted previously and then the active principle is included. The formation of the microcapsule wall occurs upon the complete coverage of the active principle by the polymers.
2. *Chemical*: The microcapsule wall is built from the polymeric reaction that occurs at the interface with the active principle (*in situ*).
3. *Physicochemical*: This process is based on the control of the solubility and precipitation conditions of the polymers. It is subject to the action of factors that may modify the solvation effect of the solvent, then promote polymer deposition over the core. Thereafter the microcapsule wall can be consolidated by means of chemical crosslinking reactions.

Table 2 - Techniques used for the production of microcapsules [66,71].

Physical	***Chemical***	***Physicochemical***
Spray drying	In situ polymerization	Simple coacervation
Spray coating	Interfacial polymerization	Complex coacervation
Fluidized bed	Emulsion crosslinking	Solvent evaporation
Lyophilization	Processes based on supercritical fluids	Molecular inclusion
Extrusion		Molecular encapsulation with cyclodextrins

The microencapsulation technique is determined according to the physicochemical characteristics of the core and shell materials, in addition to other factors such as particle

size, release mechanism, intended morphology, reproducibility and process cost, which are relevant for choosing the most appropriate microencapsulation method [36,73].

The release of the encapsulated active ingredients occurs from different mechanisms and is directly influenced by the used shell material, and the conditions of the medium into which the material is introduced [68]. The stimuli that influence the permeability of the wall material are physical (mechanical or thermal), chemical, and biological in nature [74]. Therefore the release is caused by stimuli such as friction, pressure, temperature, laser action, pH, ionic strength, solvent action, diffusion through the polymeric wall and biodegradation [11,17].

In the present work, the complex coacervation method was selected for the synthesis of microcapsules in view of its potential for large-scale industrial application, and their environmentally favorable characteristics as presented in the next topic.

2.6 Complex Coacervation

The polyelectrolytes are polymers that acquire charge when in polar aqueous solution forming coacervates. Polysaccharides are polyelectrolytes due to their ionic charges originated by the ionization of their functional groups, while proteins are polyampholytes as they have a mixture of positive and negative charges along the backbone. An example of a natural cationic polysaccharide is chitosan, which reacts by complexation with anionic polysaccharides or proteins [75].

Coacervation is the separation of a colloidal system into two phases, one in scattered state with higher colloid concentration (coacervate) resulting from electrostatic interactions between the chain of two complex biopolymers; and other with lower colloid concentration (equilibrium solution or continuous phase) [76,77]. The formation of a biphasic system occurs due to the decreased of the colloid solubility [65].

Microencapsulation by coacervation is defined as a method in which one or more biopolymers with positive or negative charges surround the active principle and form a new phase [78]. There are two classifications for coacervation: simple coacervation (SCO) and complex coacervation (CCO). The first involves the presence of only one biopolymer and one simple molecule, while the second one involves two or more opposite

charged biopolymers [76,78]. For both classifications the particle size ranges from 1-500 µm [79].

In general, CCO consists in the attraction between biopolymer molecules of opposite charges, which characterize hydrophobic interactions when they are in a low temperature aqueous solution [12,37]. In this case, the only precursor mechanism for separation between the colloidal and aqueous phase is the charge difference between the biopolymers. In contrast, in the SCO, inorganic salts are added to induce phase separation [78].

The stages of the microencapsulation process by CCO are outlined in the Figure 7. (a) Initially, droplets of the active principle are suspended in a polymer solution (b) Through pH adjustment the polymers must develop opposite charges, which might be also maximized, and interactions between both polymers result in the formation of coacervates. (c) Thus, phase separation occurs and the coacervates are deposited on the droplets of the active principle. (d) Then, there is coalescence of the droplets of coacervates forming a continuous polymeric layer around the active principle. (e) Finally, through chemical or enzymatic crosslinking, the polymeric layer can be harden in order to increase resistance [80].

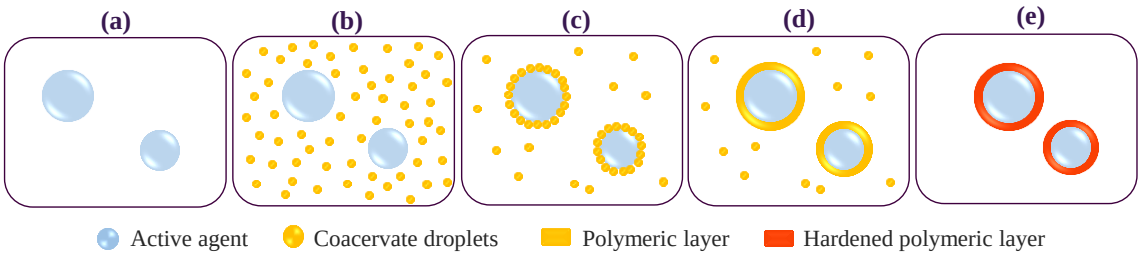

Figure 7 - Scheming of the stages of the microencapsulation process by coacervation complex. Source: Adapted from Silva *et al.* [80].

Chitosan is a cationic polymer widely used in the formation of polyelectrolytic complexes (PC) in combination with anionic polymers, such as gum Arabic. The ionic attraction, induced by the charge difference between the two polymers of high molar mass is the driving force for the formation of PC. The electrostatic interaction occur between the carboxylic groups (-COOH) present in the chemical structure of anionic polysaccharides, such as gum Arabic, and the amine groups ($-NH_2$) present in the chemical structure of chitosan (Figure 8), both ionized. The ionization of the polymers occurs when the pH of the medium is adjusted to a value close to the pK_a range of the two

polymers [81]. In the case of chitosan, ionization occurs at acidic pH, while for gum Arabic the dissociation of its carboxyl groups occurs also at acidic pH [26]. When these strong ionic interactions between polymers occur, precipitation occurs [81].

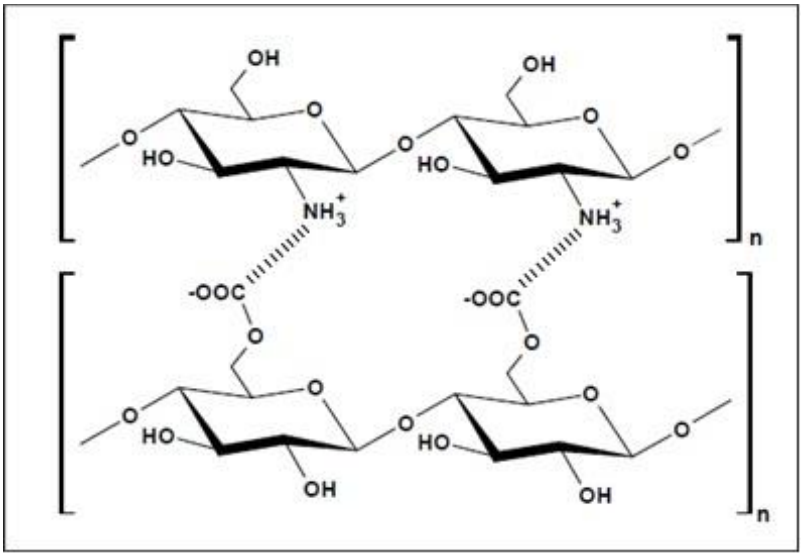

Figure 8 – Ionic interaction between the chitosan -NH_3^+ groups and -COO^- groups of an anionic polymer. Source: Adapted from Maciel [81].

Complex coacervation is one of the most widely used techniques for worldwide production of microcapsules. It is an efficient encapsulation method for water insoluble substances and is applied in the pharmaceutical, food and cosmetic industries [14,68]. The use of moderate temperatures during the coacervation processes favor the preservation of essential oils fragrance and aroma, due to their low boiling point [78].

As presented in Figure 9, Sharkawy and coworkers prepared microcapsules with chitosan and gum Arabic. In this work, the biopolymers, chitosan and gum Arabic, were previously dissolved under mechanical stirring and heated in an acetic acid solution and deionized water, respectively. In a second step, the polymeric solutions were mixed and the core material (limonene) and emulsifier added. The mixture was then emulsified at a speed of 8000 rpm at 40°C for 1 min with an Ultra-Turrax IKA DI 25 Basic. In the third step, the temperature of the mixture is lowered, from 40 to 5°C, and the pH adjusted to 3.5, to induce complex coacervation. At this step, the biopolymers acquire opposite charges and form complexes that deposit over the oil droplets. After these core-shell structures are formed, a hardening agent (tannic acid) is added to give more rigidity to the microcapsules. Finally the microcapsules, with a mean particle size of 39 μm, are separated by decantation and recovered, then they can still be washed with water [15].

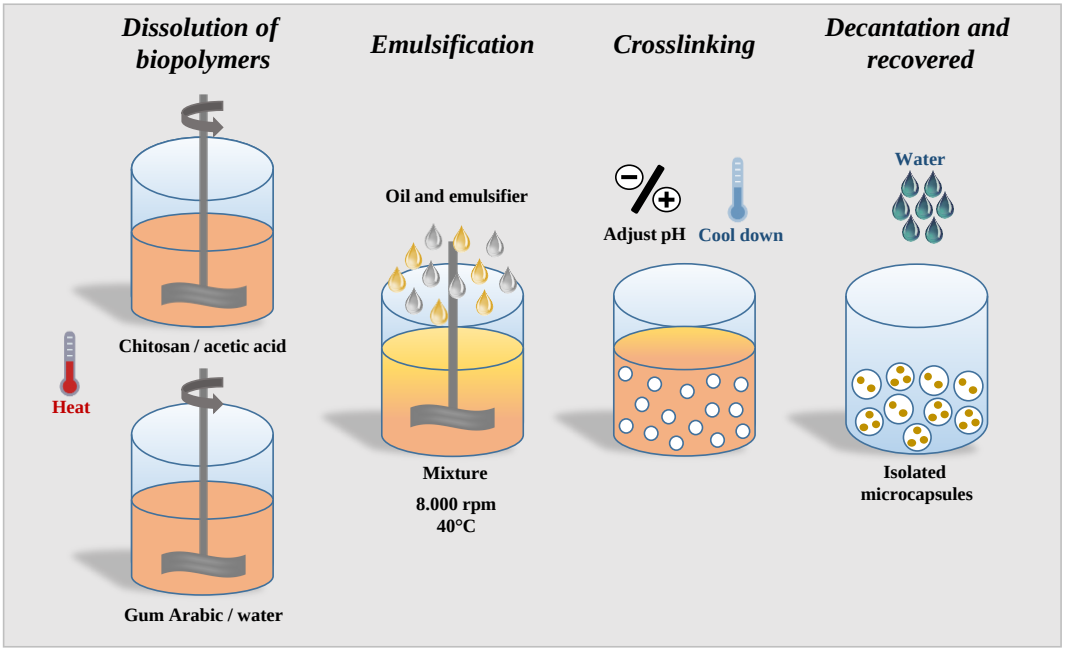

Figure 9 - Microcapsule (chitosan/gum arabic) synthesis route via complex coacervation. Source: Adapted from Sharkawy *et al.* and Carmona [15,65].

The main function of the crosslinking agent is to improve the mechanical properties of the particles. Recently, traditional hardening agents such as formaldehydes and glutaraldehydes have been replaced by new alternatives such as tannic acid (TA) due to the toxicity associated to these compounds. TA is a polyphenol of natural origin widely found in the branches and fruits of a wide variety of vegetables and belongs to the group of hydrolyzable tannins [15,82].

The chemical structure of TA comprises a glucose molecule in the center with its five hydroxyl groups esterified by two molecules of gallic acid each. Thus, the gallic acid molecules are distributed around the glucose molecule forming an organized network, as shown in Figure 10 [82,83].

The tannic acid is capable of forming hydrogen bonding and hydrophobic interactions with certain polymers, such as chitosan, for example [15]. The -OH groups present in the chemical structure of TA make hydrogen bonding with the chitosan amino groups, in addition to non-covalent interactions characteristic of complexes [84].

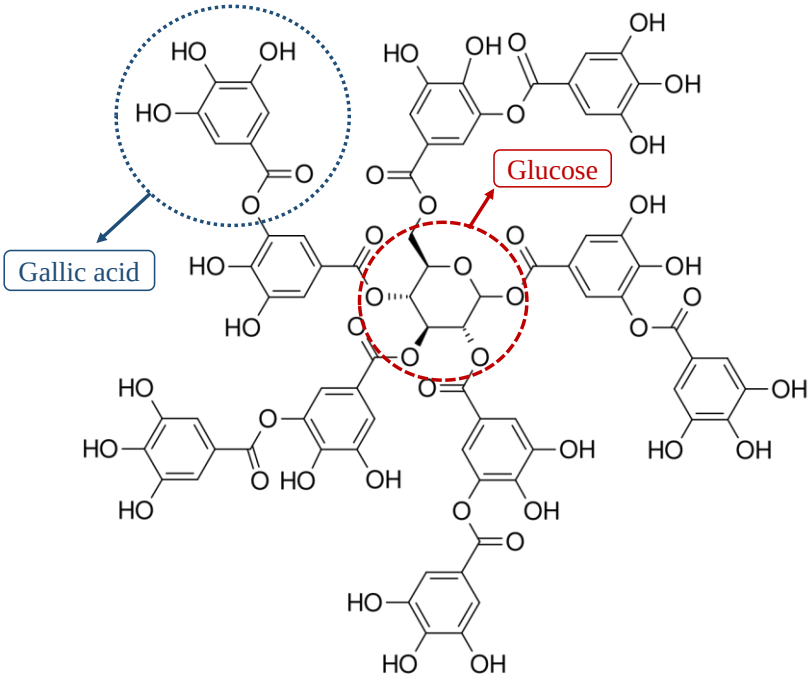

Figure 10 - Chemical structure of tannic acid.
Source: Adapted from Gülçin *et al.* [83].

Temperature and pH of the system are factors that directly influence the precipitation of the material, as well as charge change of biopolymers, respectively [37]. However, other conditions are also critical to the process, such as the type and amount of colloids, the charge ratio between both colloids, the chosen material, and physical conditions as stirring and pressure [76].

According to the characteristics previously described some advantages and disadvantages of the complex coacervation method are present in the Table 3.

Table 3 - Advantages and disadvantages of the microcapsules production for complex coacervation [6,14].

Advantages	***Disadvantages***
Use of biopolymers Absence of organic solvents Mild temperature Versatility Easy operation Scalable High encapsulation efficiency Low cost	Overuse of solvent Difficulty recovery and solubility of the active materials

The choice of the complex coacervation method for the microencapsulation process in the present work was based on the characteristics of the material to be encapsulated, in this case limonene oil, in addition to the characteristics of the capsule materials, and the experimental conditions.

2.7 Application of Microcapsules in the Textile Industry

The finishing process using functional materials in order to add or improve functional properties, besides add value to textiles, can occur through different techniques [3]. In the case of fixing microcapsules in textiles, the choice of the technique to use is an extremely important variable, because it defines the durability of the material in the textile substrate, the release behavior of the encapsulated substance, and the influence on fabric's properties [65,85].

In general, there are two possibilities of applying microcapsules to fabrics. The microcapsules can be incorporated directly into the fibers during the extrusion spinning process or in the finishing step, as shown in Figure 11. The objective in the chosen application method is to minimize the influence of microcapsule's presence on the properties of the fabric, such as touch, color, tensile strength and abrasion resistance [85,86].

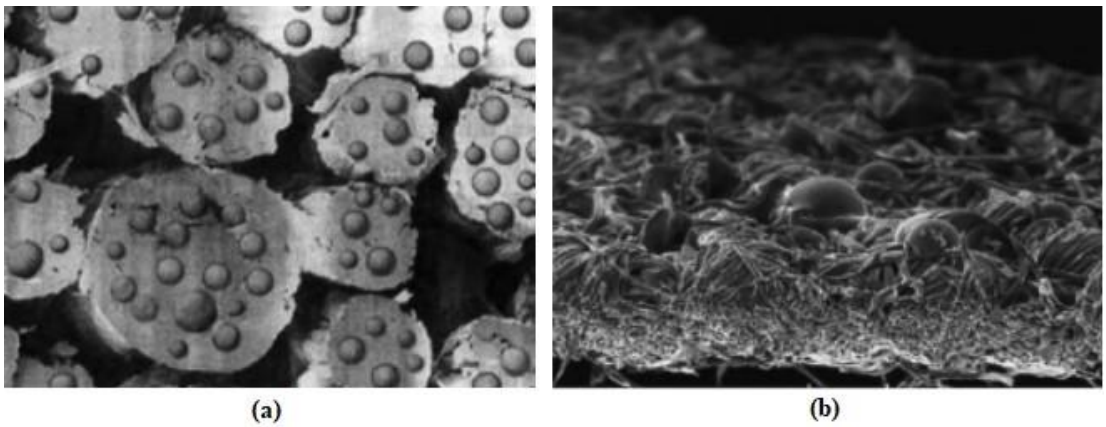

Figure 11 - **(a)** Microcapsules incorporated directly into the fiber. **(b)** Microcapsules incorporated in the finishing process.
Source: Adapted from Martín [85].

In the finishing stage, the application of microcapsules into textiles occurs through impregnation, exhaustion or coating systems, screen printing and special systems, which are briefly described below [65,87].

- *Impregnation systems*: continuous or semi-continuous mechanical process in which the fabric is immersed for a short period of time into a solution that contains the microcapsules and the finishing agent. They will be adsorbed by means of minimal differential pressure due to the hydrophilicity of the fabric [65,88].
- *Exhaustion systems*: discontinuous process in which the fabric enters into contact with the microcapsule solution for a longer period of time, usually inside a closed container. The transfer of the microcapsules to the textile substrate occurs by affinity [65].
- *Coating systems*: one or more uniform and stable layers containing microcapsules are adhered to the surface of the textile substrate [89].
- *Screen printing*: microcapsules are incorporated into the fabric by different printing techniques, such as canvas, photographic, electrostatic, pressure transfer, thermal transfer and inkjet printing [86].
- *Special systems*: the microcapsules are sprayed onto the textile substrate using a small amount of bath [65,86].

In the case of cellulosic fibers, it is common to use chemical functionalization through crosslinking reactions between the reactive groups of the polymer and the ones of the fabric [24]. Non-toxic crosslinking agents, such as citric acid and 1,2,3,4-butane-tetracarboxylic acid (BTCA), promote the esterification of the fabric facilitating the impregnation of microcapsules [15,24].

Microcapsules have the ability to provide strong adhesive strength and excellent contact with the textile substrate due to their large surface area [87]. In addition, the numerous spacing between textile fibers are an excellent deposition site for microcapsules [87]. However, the use of binders (water-soluble polymers, synthetic latex, resins and silicones) is recommended in formulations containing microcapsules in order to improve the fixation of the material onto the textile surface and, consequently, improve the durability and washability [86].

2.8 Commercial Textiles Based on Microcapsules

The emergence of microencapsulation in the textile industry occurred in 1989 when the US National Aeronautics and Space Administration (NASA) applied microcapsules to space fabrics in order to control their thermal properties [4]. Since that time, due to the numerous functionalities and potential application of microcapsules, companies from different areas have aroused interest in the material and have started to invest more in nanoscience and nanotechnology. Table 4 lists some companies that raised out the production and commercialization of functional textiles with their respective products, active agents and effects for users.

Table 4 - Companies producing functional textiles and their commercial applicability [4,90,91].

Company	Country	Core material	Textile Product	Effect
Celessence International of Hatch End	United States of America	Fragrances	Paper handkerchiefs, stationary, greeting cards, advertising brochures, books, cartons and labels	Perfume
Matsui Shikiso Chemical Co	Japan	Essences of musk, civet, green amber, pine and citrus oils	Clothes	Perfume and comfort
Eldorado International Co	South Korea	Peppermint, jasmine and orange essential oils	Curtains, sofas, pillows and sheets	Antimicrobial and aromatherapy
Aero de Celje	Slovenia	Lavender, sage and rosemary essential oils	Shoe insoles	Antimicrobial and odor control
Nocopi Technologies	United States of America	Color trainer or activator	Designer clothes	Verification of authenticity
J&C Microchem Inc.	South Korea	Paraffin	Fabrics	Temperature control
J&C Microchem Inc.	South Korea	Vitamin E	T-shirts, blouses, stockings, gloves, socks and bedding	Medicines and cosmetics
Cognis Deutschland	Germany	Shea butter, apricot kernel oil, rosehip oil and red algae extract	Sport clothes	Slimming
Micap Plc	United Kingdom	Essential oils	Bandage	Antimicrobial
THOR SARL	France	Permethrin	Military clothing	Insect repellency

Companies from North America, Europe and Eastern countries stand out in the research and production of commercial high added value textiles based on microencapsulation. The development of innovative textiles, with high quality finishes and technical performance is a lucrative alternative to an investment that was previously only intended for fiber quality [91].

Commercial textiles based on microencapsulation have several innovative properties and effects such as insect repellency, skin hydration, anti-cellulite treatments, long-lasting fragrances, drug release, vitamin release, cosmetic release, antimicrobial, water repellency, freshness, thermal control, moisture control, flame retardancy, and color changing [5,90–92]. However, it is extremely important to ensure a frequent investment in research and development of new products with a high standard of comfort, aesthetics and functionality in order to meet consumer expectations and promote the turnover in the textile market [91].

2.9 Characterization Methods

The morphology, particle size and physicochemical characteristics of the microcapsules, in addition to the study of interactions between shell material, core material and the entire encapsulation system, are analyzed using different characterization techniques, such as optical microscopy, confocal microscopy, thermogravimetric analysis, particle size evaluation, encapsulation efficiency, solid content determination, scanning electron microscopy, FT-IR spectroscopy, among others. Authors of different works in the microencapsulation area used the mentioned techniques to guarantee the functionalization and test the success of the developed microencapsulation systems.

Optical Microscopy (OM): optical microscopy is a recommended technique for analyzing colloidal systems [93]. Optical microscopy is used to check the geometry and regularity of the microcapsule walls, in addition to the effects of surfactants [94]. Surfactants directly influence particle size due to the stability provided to the system [12]. In the work developed by Rodrigues and coworkers, OM proved the spherical geometry and bimodal size distribution of the produced samples of polyurethane microcapsules containing male perfume [5].

Confocal Microscopy (CM): confocal microscopy is used when the objective is to analyze and study a specific point in the system. In this type of analysis, the high contrast of a certain point in the sample is achieved by illuminating it with greater intensity by a confocal light source [95]. In microencapsulation systems, CM is used to identify components, such as polymers, core material and surfactant, that can be marked with fluorescent dyes, in order to evaluate the capsule structure.

Thermogravimetric Analyzes (TGA): thermogravimetric analyzes are carried out in a wide temperature range, typically from ambient temperature to 600 or 700ºC, to provide information about the thermal stability of the material. Weight variation as a function of temperature is recorded continuously [96]. This type of analysis is often used to evaluate the properties and chemical stability of the polymers [94]. López and co-workers used TGA to determine the physicochemical characteristics and the presence of high and low molecular weight chitosan functional groups. In addition, from thermogravimetric analysis it was possible to analyze the influence of surfactant on the system, and identify the presence of lavender essential oil in the microcapsules [12].

Dynamic Light Scattering (DLS): dynamic light scattering is a recommended method for analyzing polymer solutions, colloidal systems and small particles [97]. This method is used to determine the size distribution of particles in the medium. DLS consists of an incidence light that spreads in different directions after reaching the microparticles. The intensity of light scattering varies with time due to the Brownian movement of the microparticles providing information about their movement and size from the detection of photons [98]. DLS provides information complementary to other characterization techniques, and has advantages such as low cost, ease of use, non-interference in the sample, and relative speed [97,99].

Encapsulation Efficiency (EE): the encapsulation efficiency is calculated from the data obtained by different characterization techniques, such as spectrophotometry, thermogravimetry and gas chromatography [5,81]. The objective of the method is to assess whether the microencapsulation process is efficient in encapsulating the core material [98]. The encapsulation system is analyzed by one or more characterization techniques in order to determine the mass percentage of the core material retained inside the capsule [5]. In the work developed by Sharkawy and co-workers, the efficiency of vanillin and limonene encapsulation in chitosan/gum Arabic capsules was determined using Equation (1) [15].

$$EE\% = \frac{mass\ (total) - mass\ (nonencapsulated)}{mass\ (total)} \times 100 \quad (1)$$

Where the $mass\ (total)$ is the total mass of the core material that was used in the process and the $mass\ (nonencapsulated)$ is the mass of the nonencapsulated core material provided by the chromatography analysis (GC-FID). This data can be also used to determine microcapsules load, an important parameter from an industrial point of view.

Solid Content Determination: the solid content determination aims to evaluate the influence of emulsifiers, and other variables, in the final product characteristics [12]. Sharkawy and co-workers determined the content of the microcapsule suspension according to European Standard EN 827 by drying 1.0 g of the sample (mass (initial)) at 100 ºC for 30 min in an oven, thereafter for 15 min in a desiccator (mass (final)), calculating the solid content from the equation (2) [15].

$$\%\ solid\ content = \frac{mass\ (final)}{mass\ (initial)} \times 100 \quad (2)$$

Scanning Electron Microscopy (SEM): scanning electron microscopy is a method used to determine the size and shape of microparticles. SEM is based on the incidence of a continuous electron beam that runs through the entire sample interacting with the atoms of the material and emitting several characteristic signals [98,101]. The signals are emitted due to excitation of the sample electrons providing details of its surface [101]. In the work of Rodrigues and co-workers, SEM was used to evaluate the effectiveness of the fixing process of polyurethane-urea microcapsules with perfume into wool and polyester fabrics [5].

Fourier-Transformed Infrared Spectroscopy (FT-IR): in microencapsulation systems, Fourier-transformed infrared spectroscopy can be used to characterize and evaluate the interaction between the polymer and the encapsulated active principle [98]. FT-IR provides spectral information at the molecular level of the sample, allowing to examine the presence of functional groups, biochemical changes and interactions between organic components [102]. FT-IR is a method for evaluating the functionality of nanoparticles. It is characterized by an easy sample preparation, quick analysis, and its

non-destructive nature [102,103]. In the work developed by Fiedler and co-workers, FT-IR-ATR spectra proved the functionalization of the cotton fabric surface with starch microcapsules by treatment with BTCA crosslinker [94].

3 MATERIALS AND METHODS

This section is devoted to the description of the materials and methods used in the present work.

3.1 Materials

The biopolymers chitosan (degree of deacetylation ≥ 90%) (Biolog-Heppe, Germany) and gum Arabic (Fisher Scientific, UK) were used as raw materials for the structural formation of the microcapsule shell. Acetic acid used for chitosan dissolution was supplied by Honeywell Fluka (Germany). Emulsifier PGPR 4125 (polyglycerol polyricinoleate) was obtained from Palsgaard (Denmark), Span 85 (sorbitane trioleate) and (R)-(+)-limonene (97%) used as core material were provided by Sigma Aldrich (USA). Hydrochloric acid was obtained from Sigma Aldrich (Germany) while tannic acid used as a hardening agent was purchased from Sigma Aldrich (China). Surfactant Triton™ was supplied by The Dow Chemical Company (USA). n-Hexane provided by Carlo Erba (Spain) was used as the solvent in the encapsulation efficiency evaluation procedure.

3.2 Methods

3.2.1 Procedure for the Microcapsule's Synthesis

The production of chitosan and gum Arabic microcapsules was based on the synthesis procedures described by Sharkawy and co-workers [15]. The microcapsule synthesis methodology is schematically represented in Figure 12. The process began with the preparation of the biopolymers aqueous solutions, chitosan and gum Arabic. The chitosan solution was prepared by adding 1 g of chitosan to 100 mL acetic acid solution (0.1 N) under mechanical stirring (400 rpm) at 40 °C for 15 h, until complete dissolution of chitosan is achieved. Similarly, the gum Arabic solution was prepared by adding 2 g of gum Arabic in 100 mL of deionized water under mechanical stirring (400 rpm) at 45 °C for 2 h, until complete dissolution of the biopolymer occurs. Next, the biopolymers solutions were mixed at 40 °C being then emulsified and (R)-(+)-limonene added. The mixture was homogenized with the Ultra-turrax Unidrive X 1000 (CAT, Germany) at 8000 rpm for a specified time. After the homogenization stage, the pH of the mixture was

adjusted to 3.5 under stirring, by adding hydrochloric acid solution (0.2 N). This step has as main objective to maximize the positive charge of chitosan (2.8 < pH < 4.0) and the negative charge of gum Arabic (pH > 2.2) [15].

Then, the mixture was placed into the jacketed batch reactor and kept under stirring at 250 rpm, being heated at 40 °C during 30 min. The resulting solution was cooled to the temperature of 5 °C, in order to promote the shell formation through the complex coacervation process. After reaching 5 °C, tannic acid aqueous solution was added drop wise to the mixture to harden the shell using an automatic pipette. This step was left to occur during 3 h. Finally, the resulting product was removed from the reactor and placed on a decantation funnel until phase separation occurred. After, in some tests, the lower phase was removed and 240 mL of deionized water was added for washing. This step was repeated twice. Thereafter the upper phase was collected and stored, being deionized water added when necessary, thus obtaining the final sample in aqueous suspension form.

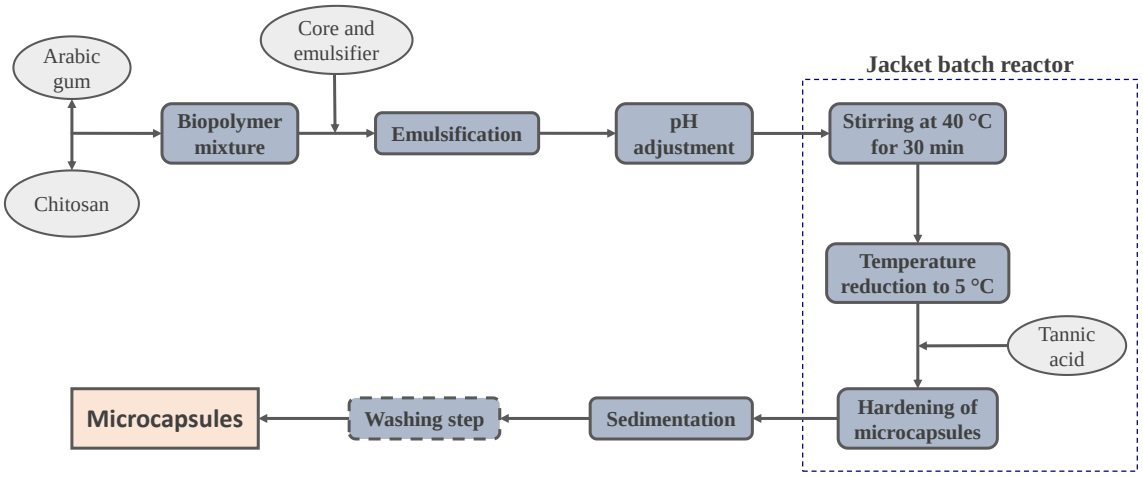

Figure 12 - Schematic representation of the microcapsules production process.

This procedure was tested at a higher scale using an experimental system composed of a jacketed batch reactor equipped with a mechanical stirrer and temperature control, as schematically represented in Figure 13. The system temperature is controlled by a thermostatized oil bath Julabo F25 (Julabo, Germany), responsible for heating and cooling the system during the synthesis process.

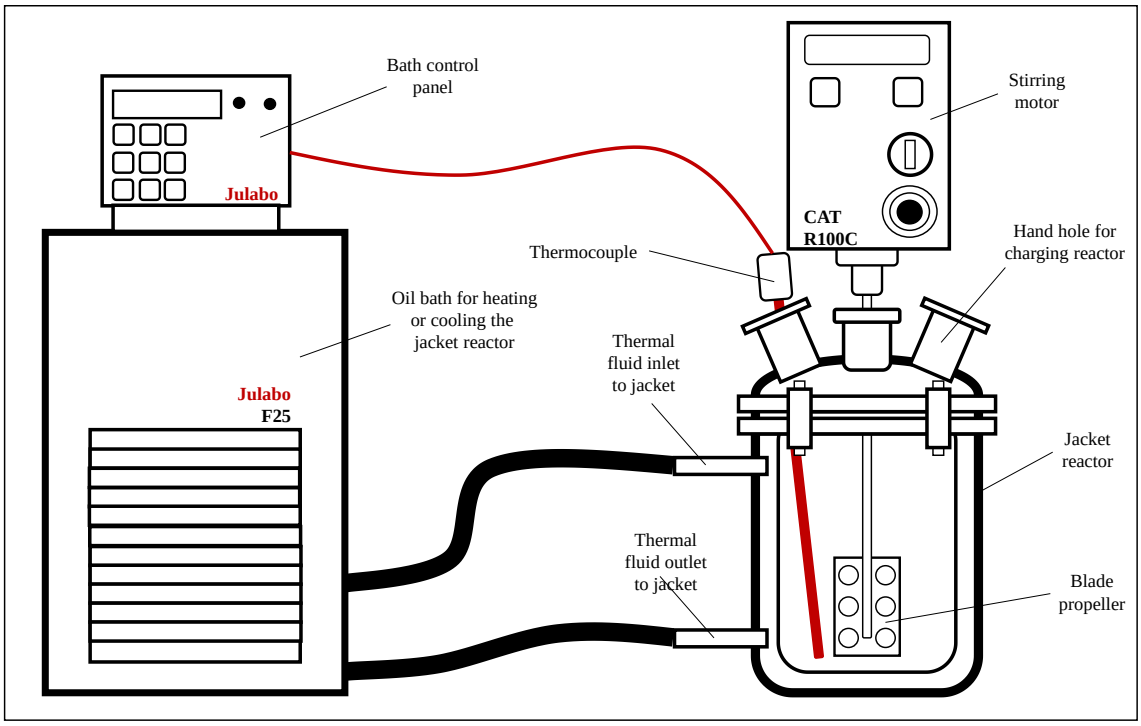

Figure 13 - Experimental scaled-up system used for the microcapsules production.

3.2.2 Characterizations of Microcapsules

3.2.2.1 Optical Microscopy

The morphology of the produced microcapsules was monitored during the synthesis stage and at the end of the process by optical microscopy. For this purpose, the analysis were performed at magnifications of 200× and 400×, using the optical microscope NiU (Nikon microscope Eclipse Ni, Nikon Corp., Japan) equipped with a digital camera and supported by the software NIS-Elements Documentation.

3.2.2.2 Solid Content

The solid content of the microcapsule suspension was determined according to the European Standard EN 827, as described by Sharkawy and co-workers [15], where a rigorous weighing of 1 g of the microcapsule suspension to a Petri dish (*initial mass*) was initially done. Then the sample was dried at 100 °C for 30 min in the oven being followed by cooling for 15 min in the desiccator. The residual mass of the sample was weighed and the sample was maintained on the desiccator until the difference between two consecutive weightings was less than 2 mg. When this criterion was achieved, the residual mass in the Petri dish was considered the *mass (final)* for determining the solids content using

Equation (2). The determination of the solids content was performed in triplicate of a single batch in two different stages, namely right after production and after the washing step with deionized water.

3.2.2.3 Particle Size Evaluation

The microcapsules particle size was evaluated in terms of volume and number distributions before and after the washing step, by laser diffraction technique (Malvern Mastersizer 3000, UK) equipped with a dispersion unit (Malvern, Hydro MV). Samples were analyzed using water as the dispersant medium and the average distributions were calculated based on five consecutive measurements.

3.2.2.4 Encapsulation Efficiency

The encapsulation efficiency was determined through the analysis of the non-encapsulated limonene recovered from the samples collected from the reactor at the end of the synthesis process, before decantation and washing steps. Then 2 mL of n-hexane and 4 mL of the mixture containing the microcapsules were mixed to prepare the sample to be analyzed. The sample was centrifuged (Eppendorf, Centrifuge 5810 R, Germany) at 3000 rpm for 5 min. The supernatant was collected and filtered through polypropylene filters, with pore diameter of 0.45 μm and 0.20 μm, in that order. The limonene content was evaluated by GC-FID using a Shimadzu Nexis 2030 gas chromatograph equipped with one OPTIMA bonded fused silica polar column (30 m×0.25 mm with 0.23 μm film thickness) and a FID detector operated by the Labsolutions software. The used method comprised setting the injector at 240 °C and the FID detector at 250 °C. The carrier gas was helium with a flow rate of 1 mL/min and a split ratio of 1:50 was used. A sample volume of 0.1 μL was injected. The measurements were carried out in triplicate and the limonene calibration curves were previously prepared.

The encapsulation efficiency (EE), in percentage, was calculated according to the Equation (1) as described by Sharkawy and co-workers [15], where the $mass\ (total)$ is the total mass of the core material that was used in the process and the $mass\ (nonencapsulated)$ is the mass of the nonencapsulated core material, in g, provided by the chromatographic analysis (GC-FID).

4 RESULTS AND DISCUSSION

4.1 Microcapsules Production Studies

The experimental procedure for producing microcapsules adopted in this work, and previously described in section **3.2.1**, was developed by Sharkawy and co-workers [15], here modified namely by using a higher experimental volume (200 mL of polymer solution) and using an experimental system enabling a more correct control of the process variables. Based on that, the first stage of the work was devoted to the microcapsules production. Here, different assays were done in order to check the parameters with higher influence in the microcapsule's properties. The process variables studied were:

1. Effect of the volume and concentration of tannic acid aqueous solution;
2. Effect of the stirring velocity used during the synthesis;
3. Homogenization step;
4. Type of emulsifier;
5. Effect of the stirring impeller design;
6. Influence of the final washing step.

A brief summary of the different formulations and experimental variables used for the systematic study devoted to the microcapsules production is described in Table 5. In total, 11 assays were carried out, being this section dedicated to the study made from assays 1 to 7, where the effect of different synthesis parameters on the generated microcapsules were studied. This evaluation was made in terms of microcapsule's morphology (analyzed by optical microscopy), and by visual inspection of the microcapsules solution.

Table 5 - Formulation and experimental conditions used in each microcapsule production assay.

Assay	Chitosan solution concentration (%, w/v)	Gum Arabic solution concentration (%, w/v)	Limonene mass (g)	Emulsifier	Emulsifier mass (g)	Homogenization step (velocity/time)	Type of stirring impeller	Stirring speed (rpm)	Tannic acid concentration (%, w/v)	Volume of tannic acid solution (mL)	Washing step/ Water volume (mL)
1	1	2	9.0	PGPR	1.2	Pre-stirring followed by homogenization (8000 rpm/2 min)	Three twisted blades	250	20	1.0	*none*
2	1	2	9.0	PGPR	1.2	Pre-stirring followed by homogenization (8000 rpm/2 min)	Three twisted blades	250	10	2.0	*none*
3	1	2	9.0	PGPR	1.2	Pre-stirring followed by homogenization (8000 rpm/2 min)	Three twisted blades	250	10	4.0	*none*
4	1	2	9.0	PGPR	1.2	Pre-stirring followed by homogenization (8000 rpm/2 min)	Three twisted blades	150	10	2.0	*none*
5	1	2	9.0	PGPR	1.2	Immediate (8000 rpm/2 min)	Three twisted blades	150	10	4.0	*none*
6	1	2	9.0	Span 85	3.15	Immediate (8000 rpm/2 min)	Three twisted blades	150	10	4.0	*none*
7	1	2	9.0	PGPR	1.2	Immediate (8000 rpm/2 min)	Two plane vertical blades	150	10	4.0	240 mL (twice)
8	1	2	9.0	PGPR	1.2	Immediate (8000 rpm/2 min)	Two plane vertical blades	150	10	4.0	240 mL (twice)
9	2	4	9.0	PGPR	1.2	Immediate (8000 rpm/2 min)	Two plane vertical blades	150	10	4.0	240 mL (twice)
10	2	4	18.0	PGPR	2.4	Immediate (8000 rpm/4 min)	Two plane vertical blades	150	10	8.0	240 mL (twice)
11	2	4	27.0	PGPR	3.6	Immediate (8000 rpm/4 min)	Two plane vertical blades	150	10	8.0	240 mL (twice)

4.1.1 Effect of the Volume and Concentration of Tannic Acid Aqueous Solution

The influence of the concentration and volume of the aqueous tannic acid solution on the morphology of the microcapsules and visual aspect of the final solution was checked in assays 1 to 3. The optical microscopy analyzes of the microcapsule synthesis process of assays 1, 2 and 3 are shown in Table A.1 of the Appendix A, using magnifications of 400x and 200x. Samples recovered from the three different process steps were analyzed, namely before adding tannic acid at 5 °C; 3 h after the addition of the tannic acid solution to the reactor; and after phase separation by decantation.

Tannic acid acts as a hardening agent of the chitosan used in the microcapsules shell. It is added to the reactional mixture shortly after the reactor temperature has reached 5 °C. The microcapsule hardening mechanism occurs through the chemical interactions occurred between the protonated amino groups (NH_3^+) of CH and the carboxyl groups of TA. The primary amine groups (NH_2) of chitosan are ionized in the presence of the carboxylic groups in the acid medium [104]. In the present work, the pH of the medium was adjusted to 3.5.

The crosslinking mechanism is further favored by the hydrogen bonding between the hydroxyl groups (OH) of TA and the protonated amino groups (NH_3^+) of CH [84]. In addition, the hydroxyl groups present in the structures of TA and CH are able to interact electronically through intermolecular hydrogen bonds. The addition of the TA at 5 °C ensures that the crosslinking of the CH occurs in a controlled manner and thus improves the thermo-mechanical properties of the microcapsules [105].

In assay 1, the formulation developed by Sharkawy and collaborators was reproduced, at a higher scale by doubling the volume of the biopolymer solutions, the oil mass and the emulsifier mass. However, in the case of the TA solution, the concentration was doubled (20% (w/v)) and the volume of 1 mL maintained as used by Sharkawy and coworkers. From the visual analysis of the produced microcapsule solution, after the phase separation in the decantation funnel, a dark brown hue was observed, as shown in Figure 14-A.

Figure 14 - Visual appearance of the microcapsules separation **(A)** in assay 1 and **(B)** in assays 2 to 6.

Due to the visual aspect reported in the first assay, a second assay was made in which the volume used of TA solution was 2 mL with a concentration of 10% (w/v). This change modified the visual aspect of the final microcapsule solution (Figure 14-B), which acquired a pink and lighter color, comparatively with that obtained in the previous assay. This same color persisted from assay 2 to assay 6. However, for assay 2 the OM analysis of the collected sample at the end of the synthesis stage, revealed the presence of spherical oil droplets surrounded by a thin polymeric layer, as it is indicated in Figure 15-A. The presence of this morphology puts in evidence the weak consolidation of the microcapsules. During the OM analyzes the rupture of these structures and the consequent oil release was observed. This problem was associated with the low volume of added TA solution, which might reacted in a heterogeneous way, before being completely mixed with the biopolymers, and thus leading to microparticles without a proper consistency and rigidity. In order to confirm this assumption, a third assay was performed, in which the volume of TA was doubled relatively to the used in assay 2, being in this case 4 mL of a solution at 10% (w/v). The OM analysis revealed the presence of less of the above mentioned structures, point out for a positive effect of the dilution of the TA solution. Despite this, the appearance of spherical structures similar to non-encapsulated oil droplets (Figure 15-B) was noticed.

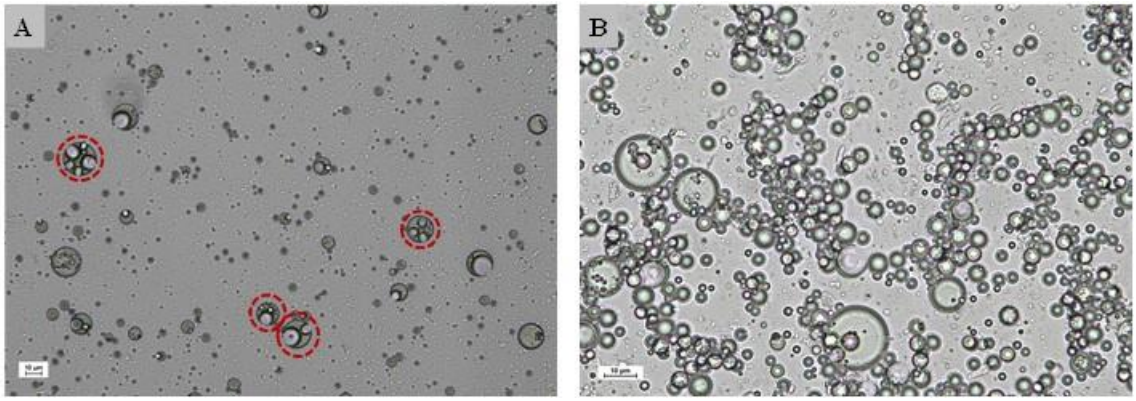

Figure 15 - OM images of **(A)** assay 2 (magnification 200×) and **(B)** assay 3 (magnification 400×) after addition of tannic acid solution and 3 h of synthesis in the reactor.

Figure 16 shows the OM analyzes of the upper (A) and lower (B) phases obtained in the decantation funnel of assays 1, 2 and 3. In this stage, water and unreacted raw materials sedimented in the funnel bottom, while the microcapsules, form a layer at the surface. The driving force for phase separation is the density difference between CH-GA particles with the encapsulated oil and the aqueous phase. At 20 °C, which was the approximate temperature used in these assays the (R)-(+)-limonene presents a density of 841.5 kg m^{-3} [106].

The OM analyzes of the upper foamed phase formed in the decantation funnel (see Figure 14), presented in Figure 16-A, revealed a large concentration of spherical and smooth particles, having a mean diameter between 1 and 10 µm. This morphology is similar to the one reported by Muhoza and collaborators for the production of gelatin and gum Arabic microcapsules, after crosslinking using TA [107]. It is important to note that the presence of a black background is due to the images acquisition mode in phase contrast mode, being done in order better visualize the microcapsules by OM.

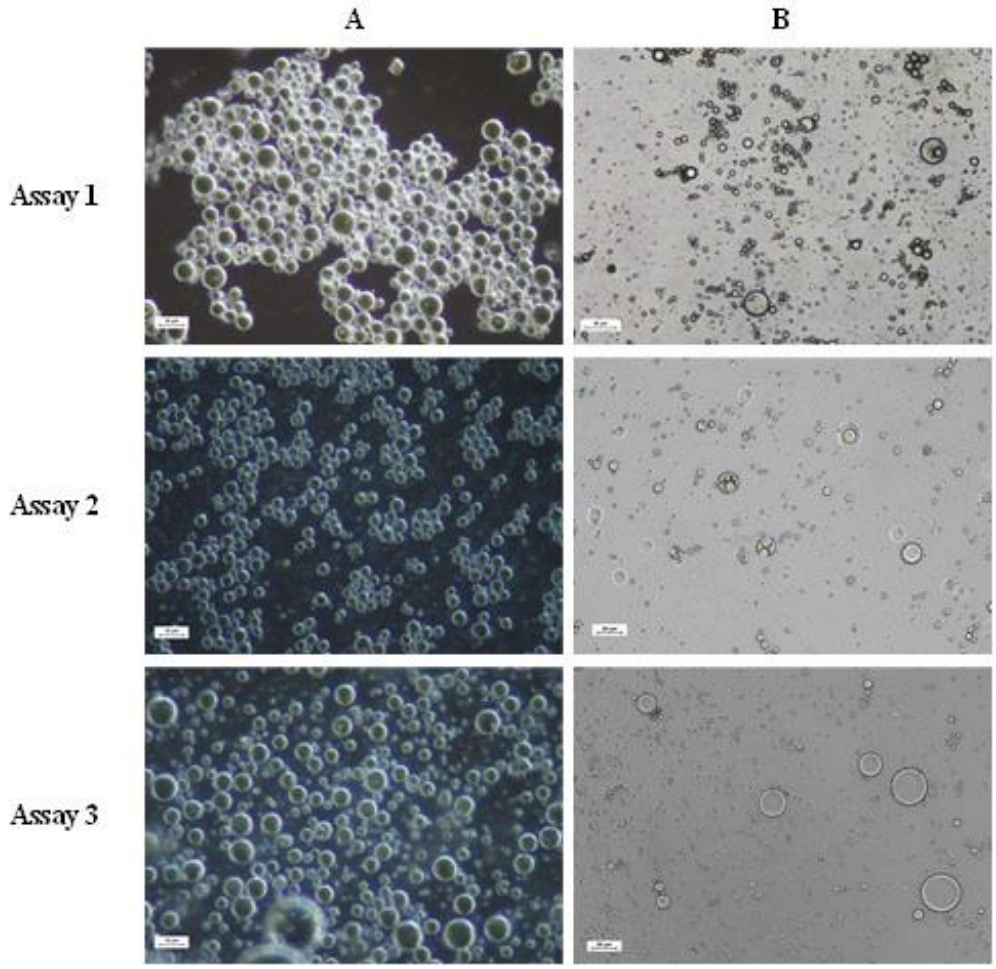

Figure 16 - OM images of the **(A)** upper phase (magnification 400×) and **(B)** lower phase (magnification 200×) obtained in the decantation funnel in assays 1, 2 and 3.

4.1.2 Effect the Stirring Rate Used During the Synthesis

Regarding the effect of the stirring rate used during the microcapsules synthesis, its influence was analyzed in assays 2 and 4. For this, the stirring rate was varied from 250 rpm in assay 2 to 150 rpm in assay 4. This reduction was done in order to analyze if this parameter as influence in the microcapsule's rupture, thus resulting on a larger amount of oil droplets dispersed in the system, as observed in the previous assays. According to Xiao and collaborators, the stirring rate used during the complex coacervation process interferes directly with the microcapsules size and morphology. Low stirring speed results in larger particles because the core material is unevenly divided. On the other hand, if the stirring rate is too high, the emulsion may break, producing irregularly shaped particles and increasing the presence of free core material [108]. In assay 4, all process variables used in assay 2 were maintained, being only reduced the stirring rate from 250 to 150

rpm. The OM analyzes of the samples recovered after the end of the synthesis and the decantation step, are presented in the Figure 17-A and Figure 17-B, respectively.

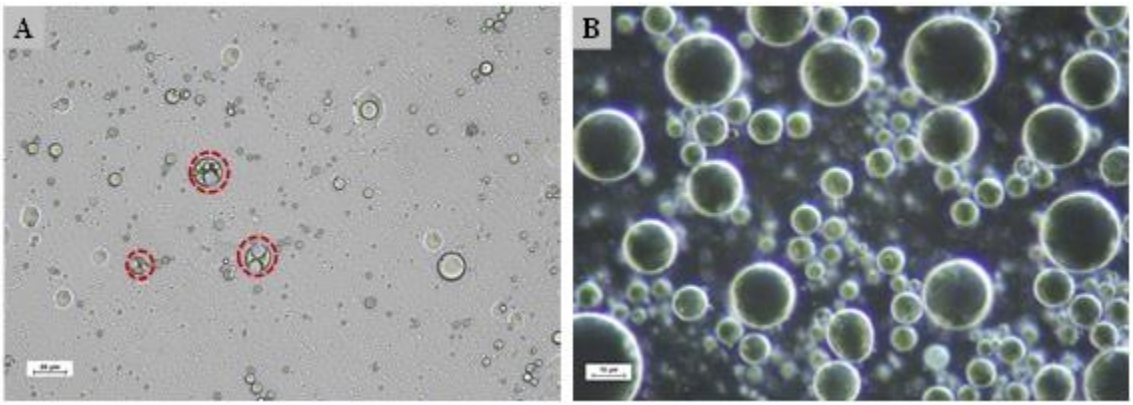

Figure 17 - OM images of assay 4 **(A)** after addition of tannic acid solution and 3 h of synthesis in the reactor (magnification 200×) and **(B)** final microcapsules sample (magnification 400×).

In Figure 17-A the presence of particles with similar morphology to those found in Figure 15-A is noted. In addition, a large number of what appears to be oil droplets are found, similarly to what was observed for assay 2 in the same step. These observations point out for a destabilization effect of the microcapsules formation driven by the high stirring rate. In contrast, when the stirring rate was lowered to 150 rpm, the degree of mixture was maintained and the generated microcapsules presented spherical structures as shown in Figure 17-B. Based on these observations, the stirring rate was maintained at 150 rpm for the following assays.

4.1.3 Homogenization Step in the Emulsion Step

Homogenization is a decisive step in the process of producing the essential oil microcapsules, since it influences the oil-in-water (o/w) emulsion formation that will rule the average size and size distribution of the formed microcapsules [108]. The homogenization is done after adding the emulsifier and the oil to the biopolymers solution. The homogenization time, stirring rate, volume ratio of the two phases and the physical-chemical properties of the chemical system are determining factors on the generated particle size [105]. In the present work, a stirring rate of 8000 rpm was used in the homogenizer. In assays 1 to 9, the homogenization was performed for 2 min, while in the assays 10 and 11 the homogenization time was increased to 4 min, due to the higher amount of used raw materials. From the assays 1 to 4, the emulsifier and core material

were added and a preliminary stirring step was done using a magnetic plate before the homogenization. In these cases, the emulsifier was firstly added under stirring at 400 rpm during 20 min being the (R)-(+)-limonene then added under stirring at 400 rpm for further 10 min. The pre-stirring step, was introduced in order to carry out a preliminary solubilization of the emulsifier and the dispersion of (R)-(+)-limonene, so that both would compounds will be more evenly distributed along the polymer solution before the homogenization step. In the subsequent assays the pre-stirring step was removed and the materials were immediately homogenized after being added to the biopolymers solution. In this case (assay 5) no considerable changes were noticed on the OM analysis (Table A.1 of Appendix A) when compared to the previous assays done with pre-stirring. Therefore, in order to reduce the overall process time and taking into account the previous considerations, the pre-stirring step of the emulsifier and oil was removed. Thus, the subsequent assays, from 5 to 11, were carried out using only the homogenization step.

4.1.4 Type of Emulsifier

The emulsifiers are compounds that reduce the surface tension by adsorption on the droplets interfaces due to their amphiphilic structure. The structural composition of an emulsifier consists of a hydrophilic head that has greater affinity with the aqueous (polar) phase and a lipophilic tail that interacts with the oily (nonpolar) phase [109]. Assays 5 and 6 were carried out using the same synthesis conditions, being only the type of emulsifier changed. The emulsifiers PGPR and Span 85 were tested in order to analyze their effects on the stability of the emulsion and dispersion of the oil droplets.

The emulsifiers PGPR and Span 85 tested in this work have a low hydrophilic-lipophilic balance (HLB) value. In numbers, PGPR's HLB ranges from 2-4 and Span 85 is close to 1.8 [15]. Emulsifiers with a low HLB value (2-6) are recommended for water-in-oil (w/o) emulsions, as they have a lipophilic character, while emulsifiers with a high HBL value (8-18) are recommended for o/w emulsions, since they have a hydrophilic character. However, the performance of the emulsifier depends not only on HLB, but also on its molecular geometry and specific interactions [110]. Therefore, in recent research studies, emulsifiers from the Span family and PGPR have been successfully used in o/w emulsions, which motivated the application of these emulsifiers in the present work.

PGPR (polyglycerol polyricinoleate) is a non-toxic and biodegradable emulsifier, obtained from the esterification of condensed fatty acids from castor oil (80-90% ricinoleic acid) with polyglycerol. PGPR's long hydrophilic polyglycerol chain guarantees excellent stability in w/o emulsions [111]. PGPR is extremely safe for human health, being classified by the FDA (Food and Drug Administration) as a GRAS (Substance Generally Recognized as Safe) [112].

Studies on emulsions based in linseed oil, carried out by Márquez and coworkers, revealed that increasing the concentration of PGPR resulted in a reduction of the interfacial tension of a w/o emulsion and improved its stability [112]. Also, according to the authors, the higher concentration of PGPR in the emulsion, 1% (w/w), and, consequently, the higher viscosity of the medium, caused a decrease in the initial size of the water droplets and a reduction of the coalescence process [112]. In the present work, a concentration of approximately 0.6% (w/w) of PGPR was used in the emulsion, while Gülseren and Corredig observed a plateau region in soybean oil-water emulsions using 0.8% (w/w) of PGPR in the oil phase [109].

Span 85, also known as sorbitane trioleate, is a small molecule nonionic emulsifier composed of hydrophobic oleic acid chains and triesters [106,109]. Yang and coworkers produced microcapsules of chitosan and gum Arabic by complex coacervation using vanillin, as the core material, and Span 83, as the o/w emulsifier, obtaining microcapsules with particle size between 5.2 and 10.3 μm [63]. In the present work, 3.15 g of Span 85 were used in an emulsion composed of 200 mL of aqueous phase and 9 mL of oil, that is, a surfactant content of 1.5% (total emulsion basis). Analyzing the emulsion samples right after the emulsification step (Figure 18-A), it is possible to identify two different droplet’s morphologies. In assay 5, in which PGPR was used, polynuclear structures are identified. In contrast, in assay 6, in which Span 85 was used, mononuclear structures are identified. These features were already expected, according to the data reported by Sharkawy and coworkers regarding the effect of the emulsifier on the microcapsules morphology [15].

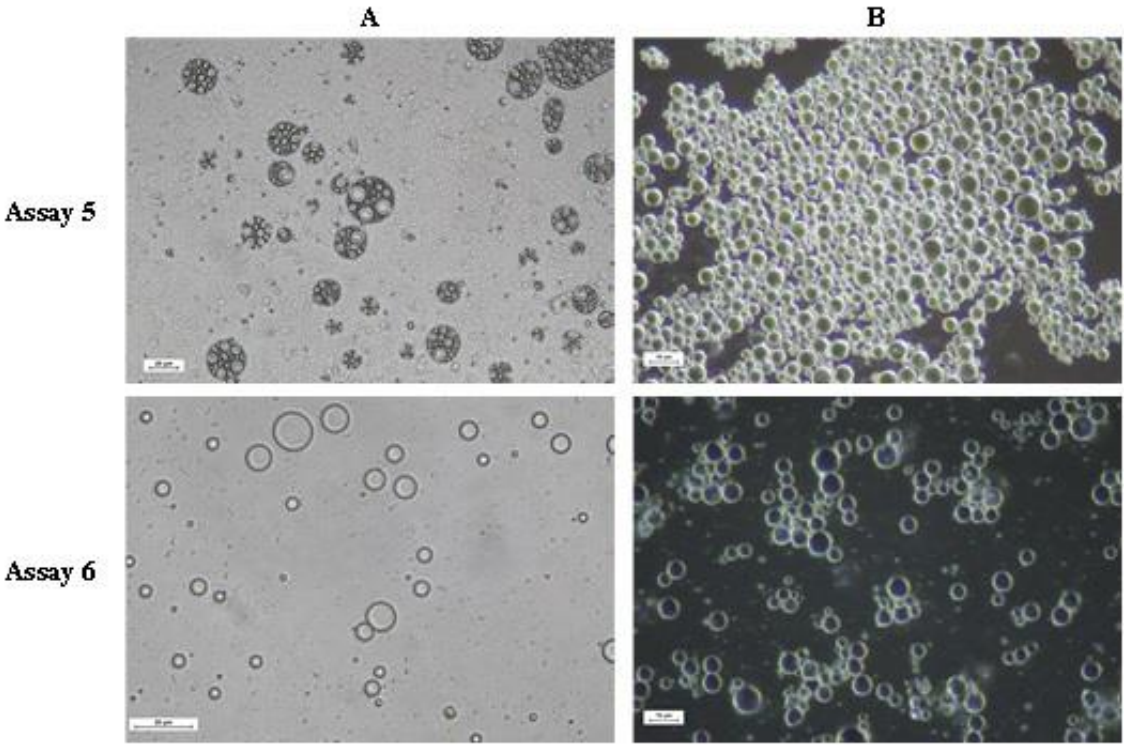

Figure 18 - OM images of assay 5 and 6 **(A)** after the emulsification step sample (magnification 200× and 400×, respectively).and **(B)** final microcapsules sample (magnification 400×).

After the emulsification, the pH correction is done in order to induce the complex coacervation. In the complex coacervation induction stage, the polymers of opposite charges, chitosan and gum Arabic are in their solubilized form and will only interact electronically and precipitate on the oil droplets due to the change in the pH of the medium to 3.5. According to Butstraen and Salaün, pH 3.6 is the optimal pH for electrostatic interaction between the two polymers, since gum Arabic is negatively charged at a pH greater than 2.2 and the positive charges of chitosan are maximized at pH between 2.8 and 4 [105]. Therefore, changing the pH is essential for the ionized groups to neutralize each other, phase separation and, consequently, complex coacervation.

In the final microcapsule samples, Figure 18-B, the poly and mononuclear morphologies are not perfectly visible, due to the addition of TA as crosslinking agent of the chitosan NH_2 groups, leading to the consolidation of the particles. Therefore, for the final sample only the presence of spherical microcapsules are observed in assays 5 and 6, without being possible to identify any differences on the morphology of the microcapsules. However, due to the successful results of the work developed by Sharkawy and coworkers, using PGPR, in addition to the characteristics already

mentioned, such as the non-toxicity character, consumer safety and biodegradability, this emulsifier was selected to proceed this study.

4.1.5 Effect of the Stirring Impeller Design

Impellers are accessories, coupled to the stirring motor, responsible for stirring and mixing, which ensure the homogeneity and uniformity of the reactive mixture [114]. Park and coworkers claim that the design of the impeller and the vessel directly influence the morphology and size of the microcapsules [115].

In the present work, two impellers with different designs were used. In a liquid-liquid mixture, the correct choice of impeller results in an increase of the stirring efficiency and, consequently, in the increase of the interfacial area [114]. This leads to an increase in the heat and mass transfer, thus contributing for the microcapsules formation to occur under suitable hydrodynamic and thermal conditions.

From the assay 1 to 6, an impeller with three twisted blades was used (Figure 19-A). This impeller promotes, predominantly, axial flow and is indicated for emulsions that have low viscosity [116]. As indicated by the arrows in Figure 19-A, the axial flow occurs parallel to the impeller axis. The liquid is moved towards the bottom of the tank and then rises up forming a single loop [114]. In the assays done using this impeller, a favorable effect was verified once both the initial and the final mixtures had a moderate viscosity. Thus, no constrains were expected from the utilization of this impeller.

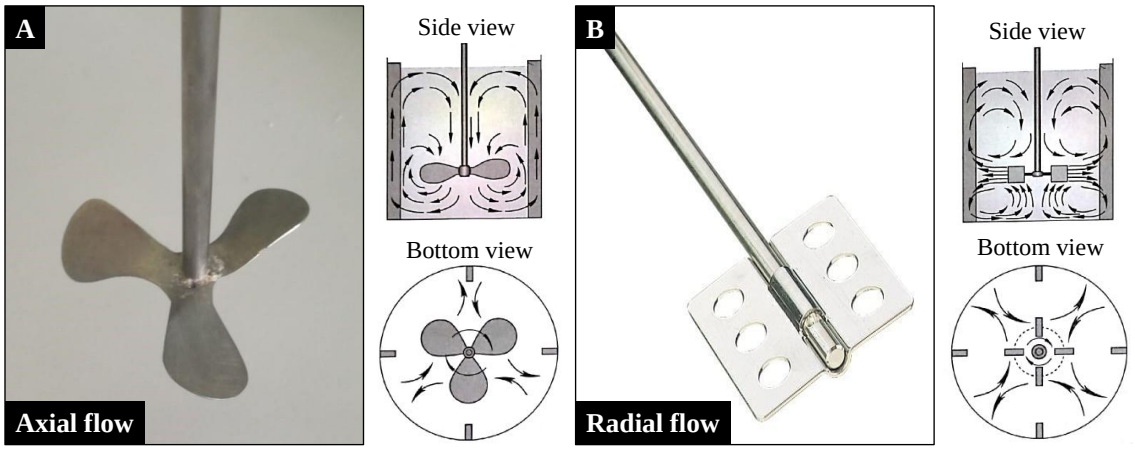

Figure 19 - Impellers tested in the microcapsule production process. **(A)** Impeller with three twisted blades. **(B)** Paddle type impeller with two flat and vertical blades.
Source: Adapted from Cremasco [116].

However, during the experimental assays, the presence of unconsolidated microcapsules and possible non-encapsulated oil droplets, even after the crosslinking step, as shown in Table A.1 in the Appendix A (samples observed after synthesis in the reactor), suggested a possible effect of the impeller type on the process. Therefore, from assays 7 to 11 other impeller, paddle type with two plane and vertical blades was used (Figure 19-B), which promotes predominantly radial flow, was used [116].

The flow promoted by this impeller is represented in Figure 19-B. The arrows indicate the fluid being dragged radially to the impeller blades, and the formation of two loop zones, one below and one above the impeller [114]. The choice of this second type of mixer was made considering the indication for low viscous systems and the promotion of good thermal exchange. In addition, it promotes less turbulent agitation, smoother than the one initially tested, being recommended for a low velocity stirring [117]. Therefore, the use of this impeller was maintained in the following assays, until assay 11, since its fluid-dynamic flow (low turbulence) is enough to maintain the uniformity of the system, promoting good thermal exchange of the mixture and no harm to the formed microcapsules.

4.1.6 Influence of the Final Washing Step

In assays 7 until 11, a final washing step of the microcapsules with 240 mL of deionized water, performed twice was adopted. The washing step starts after the first phase separation in the funnel. At this point, the lower phase obtained is completely removed, maintaining only the upper phase, which contains the highest concentration of microcapsules. The main objective of this procedure is to remove the reactants in excess from the system.

In order to inspect the composition of the lower phase obtained after the first decantation, OM analysis were performed, being the images registered in the Figure 20-A. The image shows a high concentration of solids in this phase, which consists of residual unreacted biopolymers. In addition, a larger number of spherical structures are also observed, which can be related with the presence of non-encapsulated oil droplets or small microcapsules that have not been separated from this phase.

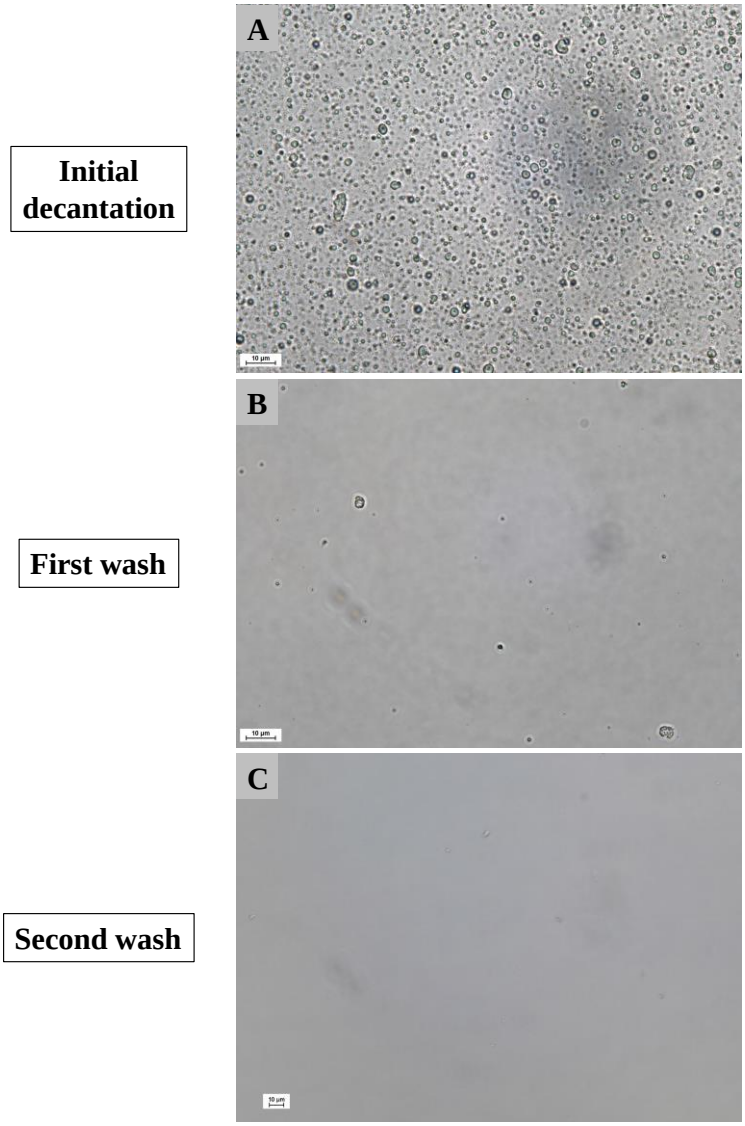

Figure 20 - OM images of the lower phase obtained in the decantation funnel of assay 7, **(A)** after initial decantation (400×), **(B)** after the first wash with water (400×), **(C)** after the second wash with water (200×).

The first wash was carried out by adding 240 mL of deionized water to the upper phase, which was kept in the funnel, promoting rapid mixing and waiting for the new phase separation. In Figure 20-B, the obtained OM analysis of the lower phase shows a concentration of solids much lower than the one obtained in the first decantation. The lower phase was again discarded, while the upper phase was kept in the funnel for a second wash.

Finally, another 240 mL of deionized water was added to the microcapsules slurry and waited for new phase separation. Again, the OM analysis of the lower phase is shown in Figure 20-C, were only few traces of solid material are seen.

The Figure 21-A, shows the visual aspect of the decantation funnel, from assay 7, after completing the washing step. In this image, the lower phase presents a clear and translucent visual aspect. Therefore, through OM analysis and the visual aspect of the lower phase, it can be concluded that the washing steps are required to remove the residual components from the microcapsules final slurry, contributing for the obtainment of a more pure final product (Figure 21-B).

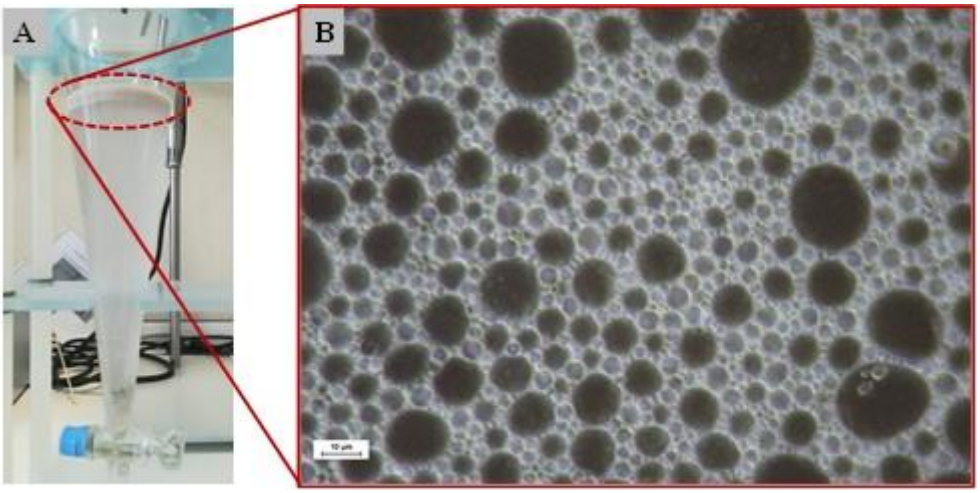

Figure 21 – **(A)** Visual aspect of the decanting funnel of assay 7 after the washing steps. **(B)** OM image of the funnel (magnification 400×).

For the subsequent assays, the analysis of the washing steps solutions were maintained. The OM imagens of the funnel lower phase are shown in Table A.2 of the Appendix A. The conclusions drawn are similar to the ones registered for assay 7, putting in evidence the importance of this additional step on the purifications of the final microcapsules.

4.2 Study of the Effect of Biopolymers Concentration and Oil Amount

In the previous section, the experimental parameters that directly influence the quality of the microcapsules produced were discussed, evaluated and adjusted in order to achieve the desired operational conditions that guarantee the required morphological characteristics. The results obtained in assay 7 were considered satisfactory, considering that the studied parameters were adjusted, thus motivating the progress of the study to a second stage, where the focus was the maximization of the microcapsules productivity. Thus, in this section, the effect of increasing the quantities of both the shell (chitosan and

gum Arabic) and core ((R)-(+)-limonene) materials was evaluated. The formulations adopted and methodological specifications of assays 8 to 11 are described in Table 6.

Table 6 - Formulation and experimental conditions used in assays 8 to 11 of microcapsule production.

Assay	Chitosan solution concentration (%, w/v)	Gum Arabic solution concentration (%, w/v)	Limonene mass (g)	PGPR mass (g)	Homogenization step (velocity/time)	Volume of tannic acid solution (mL)	Triton concentration (%, v/v)
8	1	2	9.0	1.2	(8000 rpm/2 min)	4.0	*none*
9	2	4	9.0	1.2	(8000 rpm/2 min)	4.0	*none*
10	2	4	18.0	2.4	(8000 rpm/4 min)	8.0	*none*
10 Triton	2	4	18.0	2.4	(8000 rpm/4 min)	8.0	5
11	2	4	27.0	3.6	(8000 rpm/4 min)	8.0	*none*

GA, solubilized in deionized water, has its carboxyl groups dissociated at neutral pH, resulting in an open and negatively charged molecule (groups COO^-). In contrast, CH, solubilized in acetic acid solution, has its amino groups (NH_2) protonated at acidic pH, resulting in NH_3^+ groups [118]. Therefore, from the moment the biopolymers are mixed, electrostatic interactions occur between the NH^{3+} groups of chitosan and the COO^- groups of gum Arabic.

In the work developed by Chen and collaborators, nanoparticles based on chitosan and gum Arabic were produced by complex coacervation to transport curcumin. In this work, electrostatic interactions were identified between the NH_3^+ groups of chitosan and the COO^- groups of gum Arabic by FT-IR. The FT-IR of the CH-GA nanoparticles showed important changes in the region regarding interactions between NH_3^+ and COO^-, indicating that there was an electrostatic interaction between the biopolymers in the nanoparticles [118].

First, in assay 8, the reproducibility of assay 7 was tested. In this assay, all the synthesis parameters were maintained in order to verify the results of the formulation developed in assay 7. The visual aspect of the decantation funnel in assay 8 (Figure 22-B.1) was similar to that shown in assay 7 (Figure 21-A). The upper phase, rich in microcapsules, consists of a white foamy layer that persisted even after washing with

distillated water. The lower phase, on the other hand, showed a clear appearance after the washing step, as it was noticed in assay 7.

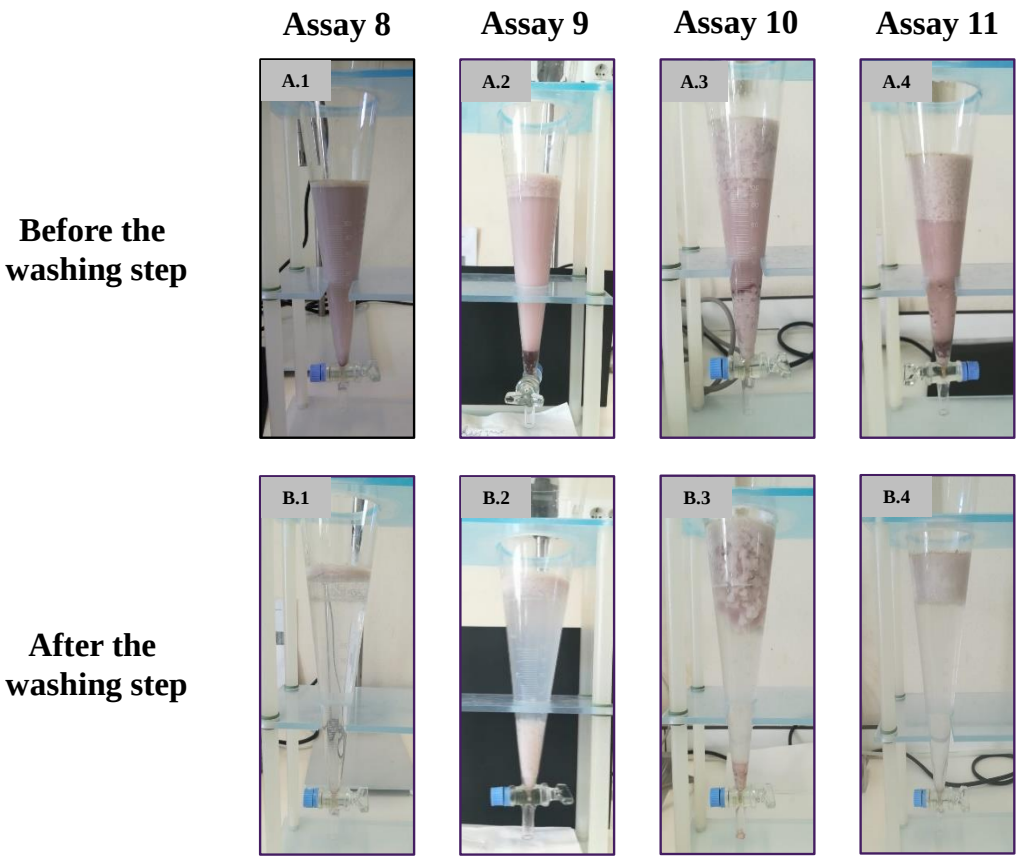

Figure 22 - Visual aspect of the decantation funnel of the assays 8 to 11, before and after the washing step.

In the case of assay 9, the concentrations of the biopolymers solutions were doubled, corresponding to 2% (w/v) of CH and 4% (w/v) of GA, while the oil mass was maintained in 9.0 g. The concentration of the biopolymer solutions was increased in order to verify an eventual increase on the amount of formed microcapsules. After the initial decantation, Figure 22-A.2, the amount of material in the upper phase increased relatively to the one in assay 8. However, after the washing step, part of the solids that were in the upper phase deposited at the bottom of the funnel (Figure 22-B.2). This indicates the presence of biopolymers in excess in the system, which were separated after washing with water. Figure 22 show the images of the decantation funnels obtained for the assays 8 to 11, after the initial decantation (A) and after the washing steps (B). Through the visual analysis of these images it is possible to identify a difference in the physical aspect of the upper phase of assay 8 comparatively with the one of assays 9 to 11. In the first case, a

layer with a foam aspect is visible, while for the assays 9 to 11 a creamy appearance is noticed.

Figure 22-A.2, corresponds to assay 9, where an amber material deposited on the bottom of the funnel can be noticed, being this visible just after the initial decantation. The OM analysis of this material (Figure 23), with magnification of 200X (A) and 400X (B), confirmed the presence of amber-colored amorphous solids in the middle of a polymeric material. The amber color is typical of tannic acid solution. This observation can be attributed to the occurrence of chemical interactions between the NH_3^+ groups of chitosan present on its free form in the system, and the hydroxyl and carbonyl groups of tannic acid, leading to the formation of these amorphous structures [83,104,107].

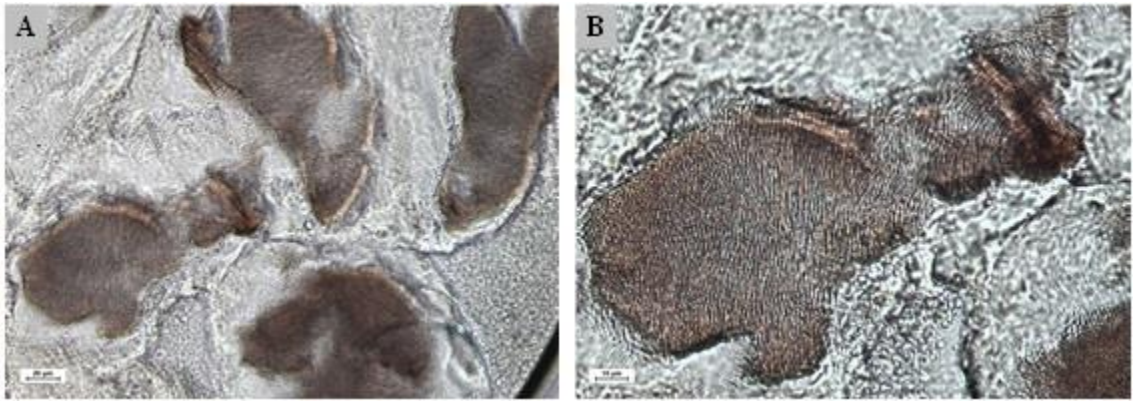

Figure 23 - OM images of the material deposited at the bottom of the funnel after the initial decantation of the microcapsules solutions from assay 9 with **(A)** magnification 200× and **(B)** magnification 400×.

In the assay 10, the mass of limonene and emulsifier were doubled, together with the concentrations of the biopolymer solutions. Thus, chitosan and gum Arabic solutions were used, at a concentration of 2% (w/v) and 4% (w/v), respectively, together with 18.0 g of (R)-(+)-limonene and 2.4 g of PGPR. Thus, the ratio of the shell to core materials remained the same as the used in assay 7, being however increased the amount of solids, in order to rise the microcapsules production.

The decantation of the microcapsules solution produced in assay 10 is shown in Figure 22-A.3, where a greater amount of solids can be identified. Part of these were on the top of the decantation funnel, while others were deposited at the bottom, even after the washing steps. This former is visible in Figure 22-B.3, corresponding to the unreacted biopolymers residues that remained at the bottom of the funnel. Figure 24 shows the OM images of the solids deposited after the initial decantation (A) and after the washing step

(B). Here the identified materials have an aspect identical to those already discussed for the assay 9 (Figure 23).

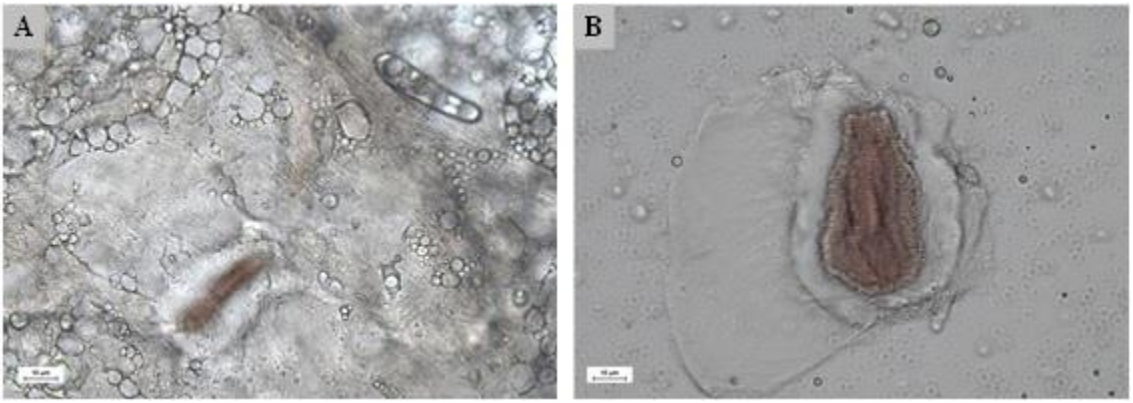

Figure 24 – OM images of the material deposited at the bottom of the funnel **(A)** after initial decantation and **(B)** after washing step of the assay 10 (magnification 400×).

In the assay 11, the mass of (R)-(+)-limonene and the emulsifier PGPR were increased 1.5 times relatively to ones used in assay 10. Thus, 27.0 g of limonene and 3.6 g of emulsifier were used. Analyzing the image of the microcapsules final solution separation show in Figure 22-A.4, an increase in the amount of the produced solids can be observed, being however also noticed the presence of deposited materials at the bottom of the funnel. Despite this, all these residues were eliminated during the washing, as it can be seen in Figure 22-B.4, where a clear aqueous phase is visible. In order to verify the composition of the removed residues, OM analyses were performed, being the obtained images shown in Figure 25-A, where a dark phase similar to the one identified in assay 9 is visible. In addition, the presence of suspended microcapsules (Figure 25-A and Figure 25-B) is observed, indicating that the microcapsules separation was not complete.

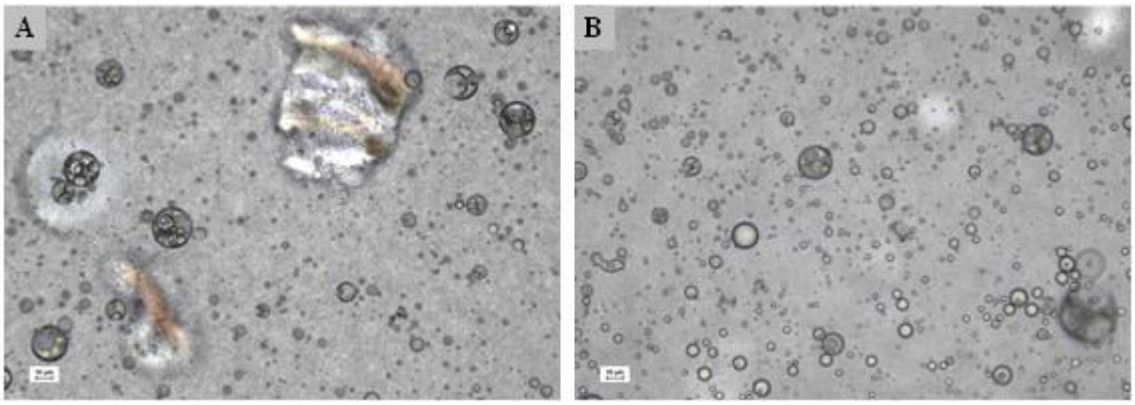

Figure 25 - OM images of the material deposited at the bottom of the funnel after initial decantation of the assay 11 (magnification 200×).

Regarding the analysis of the final microcapsules recovered from the assay 8 to 11, the OM images are shown in Figure 26.

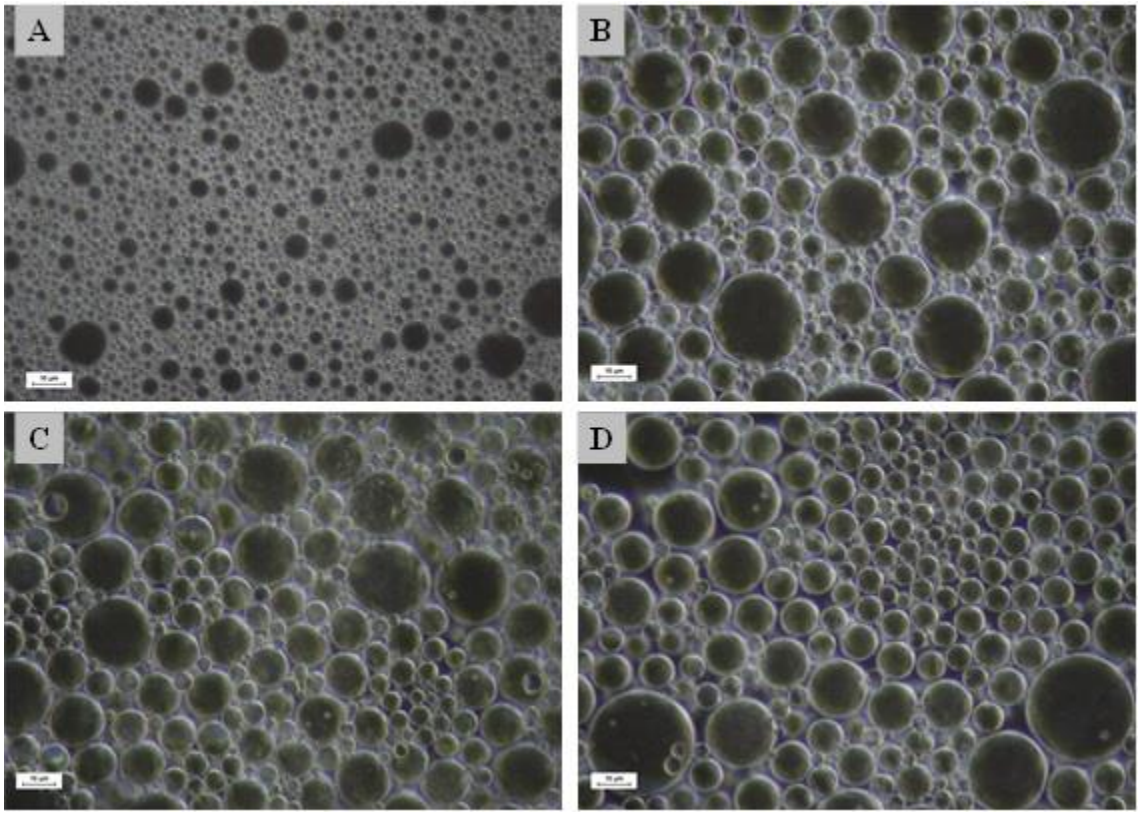

Figure 26 - OM images of final microcapsules sample from assays 8, 9, 10 and 11 (**A**, **B**, **C** and **D**, respectively) (magnification 400×).

With regard to the microcapsules produced in assay 8, the spherical conformation is predominant as it can be seen in Figure 26-A. After collecting the microcapsules, 20

mL of deionized water were added in order to obtain a more hydrated final product and thus avoid the formation of agglomerates. However, after the water addition, the formation of some microcapsules aggregates were seen, generating a heterogeneous product. These aggregates had sticky-looking solid clumps aspects, with a high concentration of microcapsules, which did not mix with water.

The images from B to D (Figure 26), correspond to the OM analysis of assays 9 to 11, respectively, were particles with spherical conformation are visible. On the surface of some microcapsules, a mildly rougher appearance is noticed, similarly to the morphologies found by Teixeira in commercial microcapsules. Microcapsules of lemon (Bayer, Focor and Horquim), strawberry (Horquim) and jasmine (Focor) also showed sphericity and a rough appearance [66]. However, most microcapsules had a smooth and uniform appearance, as shown in the OM analyzes of the microcapsules produced by Sharkawy and co-workers [15]. Regarding the particle size of assays 8 to 11, particles with an approximate size between 1 µm and 10 µm are identified.

In assay 10, 3 mL of surfactant (Triton ™) were added to 60 mL of the upper phase (corresponding to 5% (v/v)) as summarized in Table 7. Triton ™ is a non-ionic surfactant with high interfacial activity which was added to increase the microcapsules compatibility with the aqueous medium [119].

Table 7 - Data related to the amount of surfactant added to the microcapsules suspension of assay10.

Surfactant	Volume of surfactant	Volume of microcapsules suspension	Surfactant concentration in the microcapsules suspension
Triton ™	3 mL	60 mL	5% (v/v)

Figure 27 shows the OM analysis of the microcapsules added with the surfactant Triton ™. The formation of hydrophobic clusters are visible where an influence of the surfactant on the microcapsules morphology is noted. The microcapsules were surrounded by the surfactant and lost the spherical morphology found in the original sample from assay 10 (Figure 26-C). Regarding the physical aspect of the solution, the Triton ™ added microcapsules showed lower viscosity, having an aqueous aspect. Therefore, considering the previous reports, the use of the surfactant Triton was discarded, in view of its notable influence on the morphology of the microcapsules and possible negative effects on the release of the active agent.

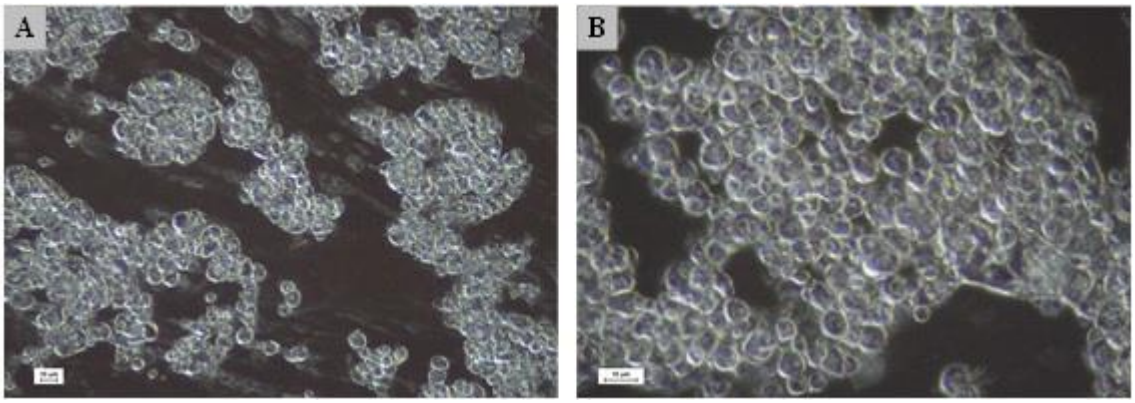

Figure 27 - Aqueous solution of the microcapsules produced in the assay 10 with addition of Triton™ (magnification **(A)** 200× and **(B)** 400×).

4.2.1 Solid Content

The solid content of the microcapsule samples, before and after the washing step, were determined, being the results obtained described in Table 8, together with the theoretical value. The theoretical value was calculated taking into account the amount of raw material added to the reactive mixture, such as biopolymers, (R)-(+)-limonene, PGPR and tannic acid.

In the samples prior to the washing step, the solids content of assay 9, was 5.68% (w/w), being the one closer the theoretical value. In contrast, in the subsequent assays, in which there was an increase of the added (R)-(+)-limonene and PGPR emulsifier, the solids content decreased, for 4.06% (w/w) and 4.35% (w/w) for assays 10 and 11, respectively.

Table 8 - Solid content before and after the washing step of the microcapsules produced in assays 8 to 11.

Assay	Solid content before the washing step (% w/w)	Solid content after the washing step (% w/w)	Theoretical solid content (% w/w)
8	2.06	14.98	5.81
9	5.68	3.77	7.09
10	4.06	2.63	11.43
11	4.35	4.21	15.08

In general, after the washing step the samples had a lower solids content in comparison with the one obtained prior to this stage, being the exception, the value registered for assay 8. In this assay, the formation of hydrophobic agglomerates occurred compromising the sampling for solids content determination. From the overall solid

content results, the decrease after the washing step is related with the elimination of the unreacted raw materials together with the unseparated microcapsules, present in the lower phase during the washes. Additionally, the final microcapsule samples from assays 9, 10 and 11 showed a more hydrated and creamy appearance. However, the washing ensures a more efficient phase separation, leading to a microcapsules higher concentration on the upper phase of the funnel.

The values of solids content obtained in the present study were lower than those determined by Sharkawy et al. for the same formulation using limonene and PGPR, 28.8% (w/w) [15]. Even with the increase of the biopolymers concentration and the (R)-(+)-limonene mass, no significant increase in the solids content was attained. This can be related to two distinct factors: (i) low oil amount which leads consequently to a low production of microcapsules; or (ii) inefficient separation of the microcapsules and dragging during the washing step. Nevertheless, this aspect can be overcome by controlling the added amount of water to the final recovered sample.

4.3 Characterization of Microcapsules

4.3.1 Particle Size Evaluation

The mean particle size of the microcapsules produced in assays 8 to 11, before and after the washing step, was evaluated by laser diffraction, being the results obtained described in Table 9. Analyzing these results, it can be observed that the microcapsules have a mean size varying from 1.92 to 2.42 μm, based on the volume distribution. These values are in the range referred in the literature for microcapsules produced by complex coacervation, which in fact comprise a very wide variation (1 and 500 μm) [79]. In addition, it was observed that the mean particle size before and after the washing step are minimal differences. This points out for an effective separation of the microcapsules with sizes closer to 1 μm or larger, being the smallest ones probably removed along the washing and decantation step.

From the perspective of the final application, microcapsules with mean particle size similar to the ones obtained herein, present better performance in textile applications. Smaller particles are fixed inside the fibers of the fabric and have better resistance to washing cycles. Monllor and co-workers studied the fixation behavior of commercial

microcapsules with a peppermint fragrance on cotton fabric and reported that smaller microcapsules remain in the fabric for more washing cycles than the larger ones [120].

Table 9 - Mean particle size (PS_{mean}) in volume and number, before and after the washing step of the microcapsules produced in the assays 8 to 11.

Assay	Before the washing step				After the washing step			
	PS_{mean} in volume (μm)	**St. Dev. ± (μm)**	**PS_{mean} in number (μm)**	**St. Dev. ± (μm)**	**PS_{mean} in volume (μm)**	**St. Dev. ± (μm)**	**PS_{mean} in number (μm)**	**St. Dev. ± (μm)**
8	1.94	0.0120	1.12	0.0040	137.00	0.5260	0.74	0.0040
9	2.36	0.0058	1.22	0.0028	2.25	0.0109	0.96	0.0026
10	2.14	0.0027	1.00	0.0009	2.42	0.0267	1.01	0.0077
10 Triton™	*	*	*	*	1.92	0.0011	0.94	0.0026
11	2.03	0.0043	0.97	0.0001	2.12	0.0072	0.93	0.0074

* Regarding data from assay 10

A study by Xiao and coworkers indicated that the increase in the stirring during the homogenization step results in a particle size increment. In the production of polynuclear microcapsules of gelatin-gum Arabic with lavender oil encapsulated by complex coacervation, a homogenization at 10000 rpm generated microcapsules with a diameter of 68.1 μm, while a homogenization at 25000 rpm generated microcapsules with 131.6 μm of diameter [108]. In the work developed by Yang and coworkers, CH-GA microcapsules with vanilla oil, formed by complex coacervation had a size variation from 5.2 to 10.3 μm when a homogenization stirring rate of 5000 rpm was used [63]. Therefore, the used homogenization speed (8000 rpm) was enough to for small-size particles.

Considering the measurements in volume described in Table 9, for the samples analyzed prior to the washing step, the mean particle size varies from 1.94 μm (assay 8) to 2.36 μm (assay 9). In the samples collected after the washing step, the smallest mean particle size is identified for assay 10, being 1.92 μm, in which surfactant (Triton ™) was added, and the largest mean size was obtained for assay 8, 137.00 μm, in which 20 mL of deionized water were added before microcapsules storage. The water addition promoted the formation of hydrophobic agglomerates with a sticky aspect that were difficult do disperse during the particle size analysis. For this reason, in this assay the particle size obtained after the washing step is higher than the obtained prior to the washing step.

The increase of the biopolymers concentration and mass of (R)-(+)-limonene, led to the variation of the core/wall material ratio, which did not impact the mean particle size of the formed microcapsules. In the work developed by Mendanha and coworkers, the tested concentrations of casein hydrolyzate (core material) also did not influence the

particle size of the microcapsules produced by complex coacervation, using soy protein and pectin as wall materials. Mendanha tested three concentrations of core material (50%, 100% and 150%) relatively to the total mass of polymers, obtaining microcapsules with little significant size variation, namely between 16.24 and 24.12 μm [121].

The particle size distribution in number and in volume of the microcapsules produced in assays 8 to 11 are presented in Table 10. Considering the volume distribution after the washing step, the peaks are centered on 1.5 μm. However, while for the sample recovered after the production the size distribution in volume is unimodal, after the washing steps became bimodal, with a second peak appearing at larger particle sizes, evidencing the formation of microcapsule's aggregates when water and Triton™ was added before storage. This trend is also identified for the final sample of the assay 10, to which Triton™ was also added, reflecting the increase of microcapsules aggregation due to this surfactant addition. For all the other samples, bimodal distributions are identified mostly after the washing step. Analyzing these results from the final application perspective, the presence of a bimodal particle size distribution is suitable for textile application, once the small particle will guarantee the long lasting effect since they will be the more resistant. The larger ones will release the core material earlier conferring the desired properties to the fabrics.

Table 10 – Particle size distribution obtained by laser diffraction, of the microcapsules produced from the assay 8 to 11, before and after the washing step.

Samples of microcapsules produced			
Assay before washing step	**Size Distribution**	**Assay after washing step**	**Size Distribution**
8	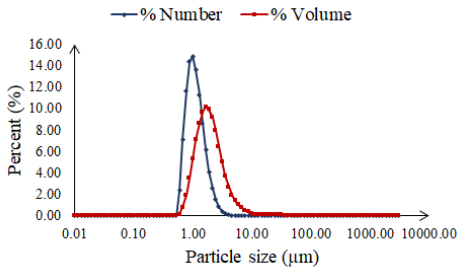	**8**	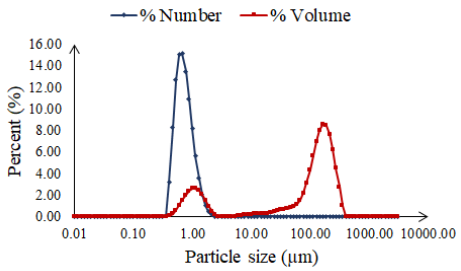
9	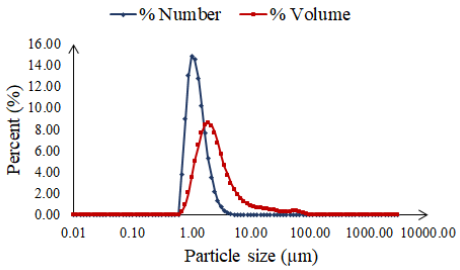	**9**	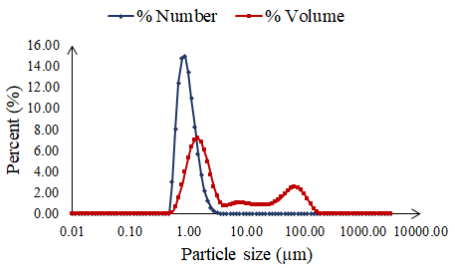
10	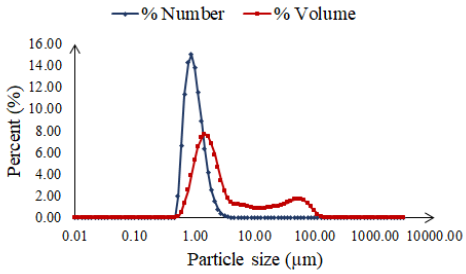	**10**	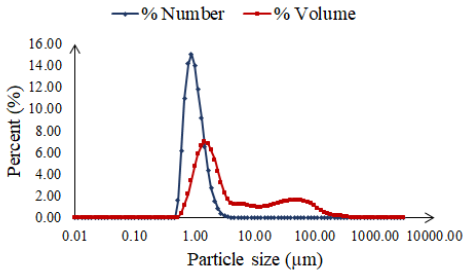
		10 Triton™	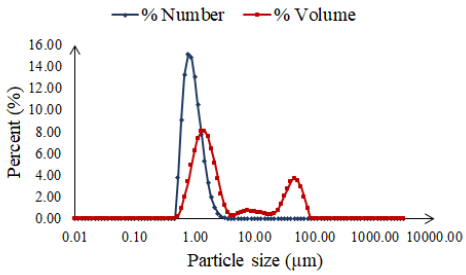
11	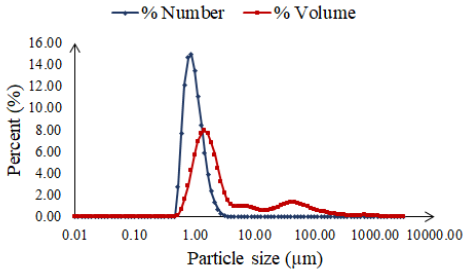	**11**	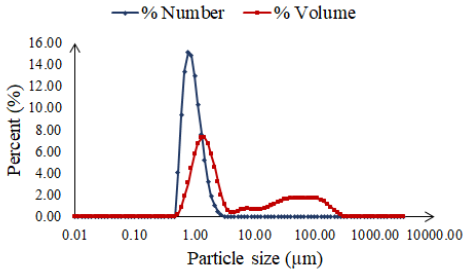

4.3.2 Encapsulation Efficiency

The encapsulation efficiency of CH-GA microcapsule samples produced in assays 9, 10 and 11 are described in Table 11. For the three analyzed samples, a high encapsulation efficiency was achieved. The results were 99.5%, 99.2% and 99.7%, for assays 9, 10 and 11, respectively, being greater than 90%, as predicted in the literature for microcapsules produced by the complex coacervation method [6,108,122]. Considering the increase of the core material added to the formulation, the EE results remained high, meaning that even in this case, the amount of biopolymers present in the reactive mixture is still enough to guarantee a good level of encapsulation.

Table 11 - Encapsulation efficiency determined for microcapsules produced in assays 9 to 11.

Assay	Encapsulation efficiency (%)
9	99.5
10	99.2
11	99.7

In the work developed by Sharkawy and co-workers, an EE of 94.1% was obtained for CH-GA microcapsules, when using the formulation containing the emulsifier PGPR and limonene, similarly to those developed in the present work. Overall, Sharkawy et al. obtained high EE in all formulations developed, between 90.4% and 100%, which is compatible with the high EE expected for the complex coacervation method herein used [15]. Butstraen and Salaün achieved an EE of 95.2% for CH-GA microcapsules produced by complex coacervation with Miglyol 812 N as the core material. This EE was found for a mass ratio of 0.25 (CH/GA) using 100 mL of NaTPP as the hardening agent [106], whereas in the present work a mass ratio of 0.5 (CH/GA) was used. The encapsulation of *Pimenta dioica* essential oil by complex coacervation using chitosan and k-carrageenan as shell materials were investigated by Dima and collaborators, obtaining high values of EE, between 92.16% and 98.31%, for microspheres with chitosan:k-carrageenan mass ratio 3:1, 3:2 and 1:1, in addition to pure chitosan [122].

Therefore, the obtained EE values are consistent with the ones mentioned on the literature for microcapsules produced by the complex coacervation method. In addition, the results point out for the presence of an excess of shell materials in the system that could encapsulate higher amounts of oil, increasing the microcapsules productivity and also the load, which is an important parameter from final application point of view.

5 CONCLUSIONS AND FUTURE WORKS

5.1 Conclusions

The present work was devoted to the production of microcapsules from an initial tested formulation, developed by the research group, and aiming at increase the scale of production and achieve a better control of the processing parameters. The used experimental apparatus was a jacketed batch reactor equipped with stirring and temperature control. Chitosan and gum Arabic were used as shell materials and (R)-(+)-limonene as the core material, having in view the development of a fully biobased system for application in the textile industry. The study was divided in the following three different sections: (i) optimization of the process variables and analysis of their influence on the microcapsule's morphology, where the influence of the homogenization stage (emulsion formation), stirring rate, geometry of the stirring impeller, volume and concentration of tannic acid solution, emulsifier type and the final washing step, was studied leading to an optimized process and reproducible; (ii) study of the biopolymers concentration and oil amount effect on process productivity; and (iii) characterization of the microcapsules produced in the last assays.

Regarding the study of the tannic acid solution concentration and volume, the assays 1 to 3 were performed. The presence of unreacted tannic acid was detected through the brownish color developed by the final reactive mixture, being proved by the OM images of the produced microcapsules. The best formulation correspond to the use of 4 mL of tannic acid solution at a concentration of 10% w/v, as used in assay 3. The produced microcapsules presented a spherical and smooth morphology without being detected an excess of tannic acid in the final solution. The evaluation of the stirring rate and the type of impeller used in the stirring, indicated that the best option was the two plane and vertical blades at 150 rpm, once these conditions ensure the appropriated fluid-dynamic flow suitable to maintain a good mixture degree of the reactive mixture, promoting a good thermal transfer and avoiding the risk of breaking the microcapsules.

Considering the emulsifier, PGPR and Span 85, two different microcapsule's morphologies were identified, being these polynuclear and mononuclear microcapsules, respectively for PGPR and Span 85. However, after adding tannic acid to the system, these morphologies became imperceptible due to the CH crosslinking mechanism and

consequent particle consolidation. As there were no significant differences, PGPR was chosen due to its non-toxicity, consumer safety and biodegradability.

During the washing step, MO monitoring of the lower phase of the decantation funnel proved its efficiency in removing the unreacted raw materials. In addition, the OM of the upper phase of the decantation funnel indicated that the spherical and smooth microcapsules remained present at high concentration after the washing step.

The solids content of the microcapsule samples produced in assays 8 to 11 were determined in order to study the effect of polymer concentration and oil mass on the productivity. Before the washing step, the solids content was 2.06%, 5.68%, 4.06% and 4.35% for the microcapsules produced in assays 8, 9, 10 and 11, respectively. After the washing step these contents were 14.98%, 3.77%, 2.63% and 4.21% for samples 8, 9, 10 and 11, respectively. Nevertheless, this aspect can be controlled since it is dependent on the added amount of water added to the final sample.

The microcapsules produced in assays 8 to 11, with different ratios between shell and core materials, were characterized in terms of particle size. In general, no significant changes in the values of their mean size before and after the washing step was noticed. The small mean particle size obtained in the 9 to 11 assays, between 1.92 and 2.42 μm, ensures a good microcapsule's performance in textile application. This is due to the small particles adhering better onto fibers and resisting longer mechanical actions.

The encapsulation efficiency of the microcapsules produced in the 9, 10 and 11 were 99.5%, 99.2% and 99.7%, respectively. The high values of EE were compatible with those found in the literature when using the complex coacervation method for microcapsule's production. The encapsulation efficiency remained high regardless of the increase in the oil mass, indicating an excess of shell material in the system in the staring formulation.

Summarizing, after performing a systematic study of the most pertinent variables, the production of limonene of CH-GA microcapsules at a scale of 200 mL and using a laboratorial reactor (capacity 1L) was successfully achieved. However, in order to achieve a high yield to guarantee the profitability at industrial level, an in-depth study of the core to shell materials ratio can be still performed.

5.2 Future Works

As future developments the following suggestions can be tested:

- Increase the solids content of the microcapsule suspension produced to guarantee high performance on an industrial scale. This can be achieved by controlling the amount of water added to the sample in the washing steps;
- Characterization of the microcapsules through SEM to better confirm their morphologies, especially in what concerns surface morphology;
- To perform FT-IR analysis to better understand the chemical interactions between the biopolymers constituting the shell;
- To do thermogravimetric analysis to evaluate the thermal stability of the microcapsules;
- To do the grafting the microcapsules onto fabrics (e.g. cotton fabrics) using the impregnation technique followed by pad-thermofixation;
- Examine by SEM the morphological characteristics of the fabric after incorporating the microcapsules;
- To perform FT-IR analysis to the treated fabrics to identify the chemical interactions between microcapsules and the fabric and to prove the effectiveness of the graft reaction;
- To perform final test of antimicrobial activity and quantify the limonene release in order to validate the functionality of the developed finished textiles.

BIBLIOGRAPHIC REFERENCE

[1] Direção Geral das Atividades Económicas, "Indústria Têxtil e Vestuário (Sinopse)," p. 26, 2018, [Online]. Available: https://www.dgae.gov.pt/gestao-de-ficheiros-externos-dgae-ano-2019/sinopse-textil-vestuario-17-04-2019-pdf.aspx.

[2] C. Cardoso and R. Pedroso, "ITV - Indústria Têxtil e de Vestuário: uma referência a nível mundial," *Port. Glob.*, vol. 113, p. 7, 2018, doi: 35783332.

[3] R. E. Meirowitz, "Coating processes and techniques for smart textiles," in *Active Coatings for Smart Textiles*, Jinlian Hu, Ed. Elsevier Ltd, 2016, pp. 159–177.

[4] G. Nelson, "Application of microencapsulation in textiles," *International Journal of Pharmaceutics*, vol. 242. pp. 55–62, 2002, doi: 10.1016/S0378-5173(02)00141-2.

[5] S. N. Rodrigues, I. M. Martins, I. P. Fernandes, P. B. Gomes, V. G. Mata, M. F. Barreiro, and A. E. Rodrigues, "Scentfashion®: Microencapsulated perfumes for textile application," *Chem. Eng. J.*, vol. 149, pp. 463–472, 2009, doi: 10.1016/j.cej.2009.02.021.

[6] E. Martins, D. Poncelet, R. C. Rodrigues, and D. Renard, "Oil encapsulation techniques using alginate as encapsulating agent: applications and drawbacks," *J. Microencapsul.*, vol. 34, no. 8, pp. 754–771, 2017, doi: 10.1080/02652048.2017.1403495.

[7] D. Alonso, M. Gimeno, J. D. Sepúlveda-Sánchez, and K. Shirai, "Chitosan-based microcapsules containing grapefruit seed extract grafted onto cellulose fibers by a non-toxic procedure," *Carbohydr. Res.*, vol. 345, pp. 854–859, 2010, doi: 10.1016/j.carres.2010.01.018.

[8] Shahid-Ul-Islam, M. Shahid, and F. Mohammad, "Perspectives for natural product based agents derived from industrial plants in textile applications - a review," *J. Clean. Prod.*, vol. 57, pp. 2–18, 2013, doi: 10.1016/j.jclepro.2013.06.004.

[9] W. P. Silvestre, N. F. Livinalli, C. Baldasso, and I. C. Tessaro, "Pervaporation in the separation of essential oil components: A review," *Trends Food Sci. Technol.*, vol. 93, pp. 42–52, 2019, doi: 10.1016/j.tifs.2019.09.003.

[10] Y. Cho, H. Kim, L. R. Beuchat, and J. H. Ryu, "Synergistic activities of gaseous

oregano and thyme thymol essential oils against Listeria monocytogenes on surfaces of a laboratory medium and radish sprouts," *Food Microbiol.*, vol. 86, p. 103357, 2020, doi: 10.1016/j.fm.2019.103357.

[11] B. Tohidi, M. Rahimmalek, and H. Trindade, "Review on essential oil, extracts composition, molecular and phytochemical properties of Thymus species in Iran," *Ind. Crops Prod.*, vol. 134, pp. 89–99, 2019, doi: 10.1016/j.indcrop.2019.02.038.

[12] A. López, M. J. Lis, F. M. Bezerra, M. Vilaseca, B. Vallés, R. Prieto, and M. Simó, "Production and Evaluation of Antimicrobial Microcapsules with Essential Oils Using Complex Coacervation," *J. Biomed. Sci. Eng.*, vol. 12, no. 8, pp. 377–390, 2019, doi: 10.4236/jbise.2019.128029.

[13] E. Ansarifar, F. Shahidi, M. Mohebbi, N. Ramezanian, A. Koocheki, and A. Mohamadian, "Optimization of limonene microencapsulation based on native and fibril soy protein isolate by VIKOR method," *LWT - Food Sci. Techlnoogy*, vol. 115, p. 107884, 2019, doi: 10.1016/j.lwt.2019.02.071.

[14] T. M. Silva, J. S. Barin, E. J. Lopes, A. J. Cichoski, E. M. M. Flores, C. B. Silva, and C. R. Menezes, "Development, characterization and viability study of probiotic microcapsules produced by complex coacervation followed by freeze-drying," *Ciência Rural*, vol. 49, no. 7, 2019, doi: 10.1590/0103-8478cr20180775.

[15] A. Sharkawy, I. P. Fernandes, M. F. Barreiro, A. E. Rodrigues, and T. Shoeib, "Aroma-Loaded Microcapsules with Antibacterial Activity for Eco-Friendly Textile Application: Synthesis, Characterization, Release, and Green Grafting," *Ind. Eng. Chem. Res.*, vol. 56, pp. 5516–5526, 2017, doi: 10.1021/acs.iecr.7b00741.

[16] A. J. Vieira, F. P. Beserra, M. C. Souza, B. M. Totti, and A. L. Rozza, "Limonene: Aroma of innovation in health and disease," *Chem. Biol. Interact.*, vol. 283, pp. 97–106, 2018, doi: 10.1016/j.cbi.2018.02.007.

[17] C. K. Padilha and G. Gomes, "Innovation culture and performance in innovation of products and processes: a study in companies of textile industry," *RAI Rev. Adm. e Inovação*, vol. 13, pp. 285–294, 2016, doi: 10.1016/j.rai.2016.09.004.

[18] M. V. O. Brasil, M. C. S. Abreu, J. C. L. S. Filho, and A. L. Leocádio, "Relationship between eco-innovations and the impact on business performance:

an empirical survey research on the Brazilian textile industry," *Rev. Adm.*, vol. 51, pp. 276–287, 2016, doi: 10.1016/j.rausp.2016.06.003.

[19] F. Noor-Evans, S. Peters, and N. Stingelin, "Nanotechnology innovation for future development in the textile industry," in *New Product Development in Textiles: Innovation and production*, 1st ed., L. Horne, Ed. Cambridge: Woodhead Publishing Limited, 2012, pp. 109–131.

[20] M. Joshi and B. Adak, "Advances in Nanotechnology Based Functional, Smart and Intelligent Textiles: A Review," in *Comprehensive Nanoscience and Nanotechnology*, 2nd ed., Elsevier Ltd., 2019, pp. 253–290.

[21] E. Moghimipour, N. Aghel, A. Z. Mahmoudabadi, Z. Ramezani, and S. Handali, "Preparation and Characterization of Liposomes Contaning Essential Oil of Eucalyptus camaldulensis Leaf," *Jundishapur J Nat Pharm Prod*, vol. 7, no. 3, pp. 117–122, 2012.

[22] E. S. Chan, Z. H. Yim, S. H. Phan, R. F. Mansa, and P. Ravindra, "Encapsulation of herbal aqueous extract through absorption with ca-alginate hydrogel beads," *Food Bioprod. Process.*, vol. 88, pp. 195–201, 2010, doi: 10.1016/j.fbp.2009.09.005.

[23] C. S. A. de Lima, "Estudo do Desenvolvimento de Microcápsulas de Polímeros Naturais para Aplicação em Têxteis Médicos," Universidade de São Paulo, 2017.

[24] P. Teixeira, "Incorporação de Quitosano em Têxteis Hospitalares Reutilizáveis," Universidade do Porto, 2015.

[25] J. Nilsen-Nygaard, S. P. Strand, K. M. Vårum, K. I. Draget, and C. T. Nordgård, "Chitosan: Gels and Interfacial Properties," *Polymers (Basel).*, vol. 7, pp. 552–579, 2015, doi: 10.3390/polym7030552.

[26] H. Rajabi, S. Mahdi, G. Rajabzadeh, and M. Sarfarazi, "Chitosan-gum Arabic complex nanocarriers for encapsulation of saffron bioactive components," *Colloids Surfaces A*, vol. 578, p. 123644, 2019, doi: 10.1016/j.colsurfa.2019.123644.

[27] Z. Ban, J. Zhang, L. Li, Z. Luo, Y. Wang, Q. Yuan, B. Zhou, and H. Liu, "Ginger essential oil-based microencapsulation as an e ffi cient delivery system for the

improvement of Jujube (Ziziphus jujuba Mill.) fruit quality," *Food Chem.*, vol. 306, p. 125628, 2020, doi: 10.1016/j.foodchem.2019.125628.

[28] M. E. Vuillemin, F. Michaux, A. A. Adam, M. Linder, and L. Muniglia, "Physicochemical characterizations of gum Arabic modified with oxidation products of ferulic acid," *Food Hydrocoll.*, vol. 107, p. 105919, 2020, doi: 10.1016/j.foodhyd.2020.105919.

[29] Ronaldo Cestari Quintanilha, "A utilização de goma arábica como agente estabilizante de nanocompósitos de poli(anilina)," Universidade Federal do Paraná, 2015.

[30] B. H. Ali, A. Ziada, and G. Blunden, "Biological effects of gum arabic: A review of some recent research," *Food Chem. Toxicol.*, vol. 47, pp. 1–8, 2009, doi: 10.1016/j.fct.2008.07.001.

[31] Y. Li, K. Han, Z. Wan, and X. Yang, "Salt reduction in semi-solid food gel via inhomogeneous distribution of sodium-containing coacervate : Effect of gum arabic," *Food Hydrocoll.*, vol. 109, p. 106102, 2020, doi: 10.1016/j.foodhyd.2020.106102.

[32] C. Zhang, Y. Li, P. Wang, J. Li, J. Weiss, and H. Zhang, "Core-shell nanofibers electrospun from O/W emulsions stabilized by the mixed monolayer of gelatin-gum Arabic complexes," *Food Hydrocoll.*, vol. 107, p. 105980, 2020, doi: 10.1016/j.foodhyd.2020.105980.

[33] M. M. Aji, S. Narendren, M. K. Purkait, and V. Katiyar, "Biopolymer (gum arabic) incorporation in waste polyvinylchloride membrane for the enhancement of hydrophilicity and natural organic matter removal in water," *J. Water Process Eng.*, vol. 38, p. 101569, 2020, doi: 10.1016/j.jwpe.2020.101569.

[34] O. Trifonova, O. Evdokimova, V. Prokofieva, and A. Matyushin, "Rationale for manufacturing of cut-pressed granules from herbal raw material rich in essential oil: An example of chamomile flowers and sweet flag rhizome," *Pharmacogn. J.*, vol. 11, no. 6, pp. 1285–1289, 2019, doi: 10.5530/pj.2019.11.199.

[35] B. Yingngam, W. Kacha, W. Rungseevijitprapa, P. Sudta, C. Prasitpuriprecha, and A. Brantner, "Response surface optimization of spray-dried citronella oil microcapsules with reduced volatility and irritation for cosmetic textile uses,"

Powder Technology, vol. 355. pp. 372–385, 2019, doi: 10.1016/j.powtec.2019.07.065.

[36] X. Sun, R. G. Cameron, and J. Bai, "Microencapsulation and antimicrobial activity of carvacrol in a pectin-alginate matrix," *Food Hydrocoll.*, vol. 92, pp. 69–73, 2019, doi: 10.1016/j.foodhyd.2019.01.006.

[37] E. F. Matos, B. S. Scopel, and A. Dettmer, "Citronella essential oil microencapsulation by complex coacervation with leather waste gelatin and sodium alginate," *J. Environ. Chem. Eng.*, vol. 6, pp. 1989–1994, 2018, doi: 10.1016/j.jece.2018.03.002.

[38] R. Timung, C. R. Barik, S. Purohit, and V. V. Goud, "Composition and anti-bacterial activity analysis of citronella oil obtained by hydrodistillation: Process optimization study," *Ind. Crops Prod.*, vol. 94, pp. 178–188, 2016, doi: 10.1016/j.indcrop.2016.08.021.

[39] R. S. Borges, B. L. S. Ortiz, A. C. M. Pereira, H. Keita, and J. C. T. Carvalho, "Rosmarinus officinalis essential oil: A review of its phytochemistry, anti-inflammatory activity, and mechanisms of action involved," *J. Ethnopharmacol.*, vol. 229, pp. 29–45, 2019, doi: 10.1016/j.jep.2018.09.038.

[40] E. M. Aldred, "Caphter 22: Terpenes," in *Pharmacology: A Handbook for Complementary Healthcare Professionals*, 1st ed., New York: Churchill Livingstone/Elsevier, 2009, pp. 167–174.

[41] H. T. Diniz-Silva, L. R. Brandão, M. S. Galvão, M. S. Madruga, J. F. Maciel, E. L. Souza, and M. Magnani, "Survival of Lactobacillus acidophilus LA-5 and Escherichia coli O157:H7 in Minas Frescal cheese made with oregano and rosemary essential oils," *Food Microbiol.*, vol. 86, p. 103348, 2020, doi: 10.1016/j.fm.2019.103348.

[42] G. Maria, B. Zinaida, S. Tatiana, R. Gabriela, and G. Natalia, "Essential Oil of Origanum vulgare ssp. vulgare L. and Origanum vulgare ssp. hirtum (Link) Ietswaart from Moldova: Content and Chemical Composition," *Int. J. Agric. Innov. Res.*, vol. 3, no. 2, pp. 659–663, 2014.

[43] H. Cui, C. Zhang, C. Li, and L. Lin, "Antibacterial mechanism of oregano essential oil," *Ind. Crops Prod.*, vol. 139, p. 111498, 2019, doi:

10.1016/j.indcrop.2019.111498.

[44] C. Takayama, F. M. de-Faria, A. C. A. Almeida, R. J. Dunder, L. P. Manzo, E. A. R. Socca, L. M. Batista, M. J. Salvador, A. R. M. Souza-Brito, and A. Luiz-Ferreira, "Chemical composition of Rosmarinus officinalis essential oil and antioxidant action against gastric damage induced by absolute ethanol in the rat," *Asian Pac. J. Trop. Biomed.*, vol. 6, no. 8, pp. 677–681, 2016, doi: 10.1016/j.apjtb.2015.09.027.

[45] F. M. Bezerra, M. Lis, O. G. Carmona, C. G. Carmona, M. P. Moisés, G. M. Zanin, and F. F. Moraes, "Assessment of the delivery of citronella oil from microcapsules supported on wool fabrics," *Powder Technol.*, vol. 343, pp. 775–782, 2019, doi: 10.1016/j.powtec.2018.11.001.

[46] H. M. A. Cavanagh and J. M. Wilkinson, "Lavender essential oil: a review," *Aust. Infect. Control*, vol. 10, no. 1, pp. 35–37, 2005, doi: 10.1071/hi05035.

[47] C. Yuan, Y. Wang, Y. Liu, and B. Cui, "Physicochemical characterization and antibacterial activity assessment of lavender essential oil encapsulated in hydroxypropyl-beta-cyclodextrin," *Ind. Crops Prod.*, vol. 130, pp. 104–110, 2019, doi: 10.1016/j.indcrop.2018.12.067.

[48] M. Adaszýnska-Skwirzýnska and D. Szczerbínska, "The effect of lavender (Lavandula angustifolia) essential oil as a drinking water supplement on the production performance, blood biochemical parameters, and ileal microflora in broiler chickens," *Poult. Sci.*, vol. 98, no. 1, pp. 358–365, 2019, doi: 10.3382/ps/pey385.

[49] G. Giunti, D. Palermo, F. Laudani, G. M. Algeri, O. Campolo, and V. Palmeri, "Repellence and acute toxicity of a nano-emulsion of sweet orange essential oil toward two major stored grain insect pests," *Ind. Crops Prod.*, vol. 142, p. 111869, 2019, doi: 10.1016/j.indcrop.2019.111869.

[50] J. A. Evangelho, G. S. Dannenberg, B. Biduski, S. L. M. Halal, D. H. Kringel, M. A. Gularte, A. M. Fiorentini, and E. R. Zavareze, "Antibacterial activity, optical, mechanical, and barrier properties of corn starch films containing orange essential oil," *Carbohydr. Polym.*, vol. 222, p. 114981, 2019, doi: 10.1016/j.carbpol.2019.114981.

[51] D. Li, H. Wu, H. Dou, L. Guo, and W. Huang, "Microcapsule of sweet orange essential oil changes gut microbiota in diet-induced obese rats," *Biochem. Biophys. Res. Commun.*, vol. 505, no. 4, pp. 991–995, 2018, doi: 10.1016/j.bbrc.2018.10.035.

[52] B. Asghari, G. Zengin, M. B. Bahadori, M. Abbas-Mohammadi, and L. Dinparast, "Amylase, glucosidase, tyrosinase, and cholinesterases inhibitory, antioxidant effects, and GC-MS analysis of wild mint (Mentha longifolia var. calliantha) essential oil: A natural remedy," *Eur. J. Integr. Med.*, vol. 22, pp. 44–49, 2018, doi: 10.1016/j.eujim.2018.08.004.

[53] V. Nazem, M. R. Sabzalian, G. Saeidi, and M. Rahimmalek, "Essential oil yield and composition and secondary metabolites in self- and open-pollinated populations of mint (Mentha spp.)," *Ind. Crops Prod.*, vol. 130, pp. 332–340, 2019, doi: 10.1016/j.indcrop.2018.12.018.

[54] S. Secouard, C. Malhiac, M. Grisel, and B. Decroix, "Release of limonene from polysaccharide matrices: viscosity and synergy effect," *Food Chem.*, vol. 82, pp. 227–234, 2003, doi: 10.1016/S0308-8146(02)00518-6.

[55] K. Faure, E. Bouju, P. Suchet, and A. Berthod, "Limonene in Arizona liquid systems used in countercurrent chromatography. i physicochemical properties," *Anal. Bioanal. Chem.*, vol. 406, no. 24, pp. 5909–5917, 2014, doi: 10.1007/s00216-014-8005-3.

[56] A. K. Antosik, K. Wilpiszewska, A. Wróblewska, A. Markowska-Szczupak, and M. W. Malko, "Fragrant starch-based films with limonene," *Curr. Chem. Lett.*, vol. 6, no. 2, pp. 41–48, 2017, doi: 10.5267/j.ccl.2017.2.002.

[57] W. O. Chemicals, "Potential Health Benefits of Limonene." https://www.worldofchemicals.com/518/chemistry-articles/potential-health-benefits-of-limonene.html.

[58] F. Chemat, M. Abert-Vian, A. S. Fabiano-Tixier, J. Strube, L. Uhlenbrock, V. Gunjevic, and G. Cravotto, "Green extraction of natural products. Origins, current status, and future challenges," *Trends Anal. Chem.*, vol. 118, pp. 248–263, 2019, doi: 10.1016/j.trac.2019.05.037.

[59] A. Prakash, R. Baskaran, N. Paramasivam, and V. Vadivel, "Essential oil based

nanoemulsions to improve the microbial quality of minimally processed fruits and vegetables: A review," *Food Res. Int.*, vol. 111, pp. 509–523, 2018, doi: 10.1016/j.foodres.2018.05.066.

[60] N. J. Zuidam and V. A. Nedovic, *Encapsulation technologies for active food ingredients and food processing*. New York: Springer Science, 2010.

[61] S. Krishnan, A. C. Kshirsagar, and R. S. Singhal, "The use of gum arabic and modified starch in the microencapsulation of a food flavoring agent," *Carbohydr. Polym.*, vol. 62, no. 4, pp. 309–315, 2005, doi: 10.1016/j.carbpol.2005.03.020.

[62] S. Mondal, "Phase change materials for smart textiles - An overview," *Appl. Therm. Eng.*, vol. 28, pp. 1536–1550, 2008, doi: 10.1016/j.applthermaleng.2007.08.009.

[63] Z. Yang, Z. Peng, J. Li, S. Li, L. Kong, P. Li, and K. Wang, "Development and evaluation of novel flavour microcapsules containing vanilla oil using complex coacervation approach," *Food Chem.*, vol. 145, pp. 272–277, 2014, doi: 10.1016/j.foodchem.2013.08.074.

[64] W. Yang, L. Wang, Z. Ban, J. Yan, H. Lu, X. Zhang, Q. Wu, M. S. Aghdam, Z. Luo, and L. Li, "Efficient microencapsulation of Syringa essential oil; the valuable potential on quality maintenance and storage behavior of peach," *Food Hydrocoll.*, vol. 95, pp. 177–185, 2019, doi: 10.1016/j.foodhyd.2019.04.033.

[65] C. G. Carmona, "Desarollo de microcápsulas rígidas de fragancia y de técnicas que permitan la cuantificación de la eficiencia de encapsulación," Universitat Politècnica de Catalunya, 2019.

[66] C. S. Nogueira Rodrigues Teixeira, "Microencapsulation of Perfumes For Application in Textile Industry," University of Porto, 2010.

[67] S. Ghayempour and M. Montazer, "Micro/nanoencapsulation of essential oils and fragrances: Focus on perfumed, antimicrobial, mosquito-repellent and medical textiles," *J. Microencapsul.*, vol. 33, no. 6, pp. 497–510, 2016, doi: 10.1080/02652048.2016.1216187.

[68] S. Y. Cheng, C. W. M. Yuen, C. W. Kan, and K. K. L. Cheuk, "Development of Cosmetic Textiles Using Microencapsulation Technology," *Res. J. Text. Appar.*,

vol. 12, no. 4, pp. 41–51, 2008, doi: 10.1108/rjta-12-04-2008-b005.

[69] L. Le Priol, A. Dagmey, S. Morandat, K. Saleh, K. El Kirat, and A. Nesterenko, "Comparative study of plant protein extracts as wall materials for the improvement of the oxidative stability of sunflower oil by microencapsulation," *Food Hydrocoll.*, vol. 95, pp. 105–115, 2019, doi: 10.1016/j.foodhyd.2019.04.026.

[70] S. S. Bansode, S. K. Banarjee, D. D. Gaikwad, S. L. Jadhav, and R. M. Thorat, "Microencapsulation: A review," *Int. J. Pharm. Sci. Rev. Res.*, vol. 1, no. 2, pp. 38–43, 2010.

[71] F. Dutra, M. J. Lis, C. García, A. Plath, F. Scacchetti, and F. M. Bezerra, "Microencapsulation of C.I. reactive Orange 122 via solvent evaporation," *AUTEX 2019 – 19th World Textile Conference on Textiles at the Crossroads*, Ghent, 2019.

[72] L. R.G. Kumar, N. S. Chatterjee, C. S. Tejpal, K. V. Vishnu, K. K. Anas, K. K. Asha, R. Anandan, and S. Mathew, "Evaluation of chitosan as a wall material for microencapsulation of squalene by spray drying: Characterization and oxidative stability studies," *Int. J. Biol. Macromol.*, vol. 104, pp. 1986–1995, 2017, doi: 10.1016/j.ijbiomac.2017.03.114.

[73] M. J. L. Arias, L. Coderch, M. Martí, C. Alonso, O. G. Carmona, C. G. Carmona, and F. Maestá, "Vehiculation of active principles as a way to create smart and biofunctional textiles," *Materials (Basel).*, vol. 11, p. 2152, 2018, doi: 10.3390/ma11112152.

[74] M. Delcea, H. Möhwald, and A. G. Skirtach, "Stimuli-responsive LbL capsules and nanoshells for drug delivery," *Adv. Drug Deliv. Rev.*, vol. 63, no. 9, pp. 730–747, 2011, doi: 10.1016/j.addr.2011.03.010.

[75] H. Espinosa-Andrews, C. Lobato-Calleros, J. M. Loeza-Corte, C. I. Beristain, M. E. Rodríguez-Huezo, and E. J. Vernon-Carter, "Quantification of the composition of gum arabic-chitosan coacervates by hplc," *Rev. Mex. Ing. Qum.*, vol. 7, no. 3, pp. 293–298, 2008.

[76] C. G. De Kruif, F. Weinbreck, and R. De Vries, "Complex coacervation of proteins and anionic polysaccharides," *Curr. Opin. Colloid Interface Sci.*, vol. 9, no. 5, pp. 340–349, 2004, doi: 10.1016/j.cocis.2004.09.006.

[77] Y. P. Timilsena, B. Wang, R. Adhikari, and B. Adhikari, “Advances in microencapsulation of polyunsaturated fatty acids (PUFAs)-rich plant oils using complex coacervation: A review,” *Food Hydrocoll.*, vol. 69, pp. 369–381, 2017, doi: 10.1016/j.foodhyd.2017.03.007.

[78] Z. Xiao, W. Li, and G. Zhu, “Effect of wall materials and core oil on the formation and properties of styralyl acetate microcapsules prepared by complex coacervation,” *Colloid Polym. Sci.*, vol. 293, no. 5, pp. 1339–1348, 2015, doi: 10.1007/s00396-015-3515-x.

[79] R. Meirowitz, “Microencapsulation technology for coating and lamination of textiles,” in *Smart Textile Coatings and Laminates*, Woodhead Publishing Limited, 2010, pp. 125–154.

[80] T. M. da Silva, L. Z. Rodrigues, C. F. Codevilla, C. Bona, and C. R. De Menezes, “Coacervação complexa : uma técnica para a encapsulação de probióticos,” *Ciência e Nat.*, vol. 37, pp. 49–55, 2015, doi: 10.5902/2179-460X19714.

[81] J. da S. Maciel, “Géis de Goma do Cajueiro e Derivados Com Quitosana: Síntese, Caracterização e Ensaios Preliminares em Sistemas de Liberação de Fármacos,” Universidade Federal do Ceará, 2005.

[82] G. K. B. Lopes, H. M. Schulman, and M. Hermes-Lima, “Polyphenol tannic acid inhibits hydroxyl radical formation from Fenton reaction by complexing ferrous ions,” *Biochim. Biophys. Acta*, vol. 1472, pp. 142–152, 1999.

[83] I. Gülçin, Z. Huyut, M. Elmastaş, and H. Y. Aboul-Enein, “Radical scavenging and antioxidant activity of tannic acid,” *Arab. J. Chem.*, vol. 3, no. 1, pp. 43–53, 2010, doi: 10.1016/j.arabjc.2009.12.008.

[84] X. An, Y. Kang, and G. Li, “The interaction between chitosan and tannic acid calculated based on the density functional theory,” *Chem. Phys.*, vol. 520, pp. 100–107, 2019, doi: 10.1016/j.chemphys.2018.12.009.

[85] J. R. Sánchez Martín, “Los tejidos inteligentes y el desarrollo tecnológico de la industria textil,” *Técnica Ind. 268*, pp. 38–45, 2007, [Online]. Available: http://www.tecnicaindustrial.es/tiadmin/numeros/28/36/a36.pdf.

[86] B. P. Bojana and S. Marica, “Microencapsulation technology and applications in

added-value functional textiles," *Phys. Sci. Rev.*, 2016, doi: 10.1515/psr-2015-0003.

[87] J. Liu, C. Liu, Y. Liu, M. Chen, Y. Hu, and Z. Yang, "Study on the grafting of chitosan-gelatin microcapsules onto cotton fabrics and its antibacterial effect," *Colloids and Surfaces B: Biointerfaces*, vol. 109. pp. 103–108, 2013, doi: 10.1016/j.colsurfb.2013.03.040.

[88] M. Zahid, G. Mazzon, A. Athanassiou, and I. S. Bayer, "Environmentally benign non-wettable textile treatments: A review of recent state-of-the-art," *Adv. Colloid Interface Sci.*, vol. 270, pp. 216–250, 2019, doi: 10.1016/j.cis.2019.06.001.

[89] E. Shim, "Coating and laminating processes and techniques for textiles," in *Smart Textile Coatings and Laminates*, 2010, pp. 10–41.

[90] S. Siler-Marinkovic, D. Bezbradica, and P. Skundric, "Microencapsulation in the textile industry," *Chem. Ind. Chem. Eng. Q.*, vol. 12, no. 1, pp. 58–62, 2006, doi: 10.2298/ciceq0601058s.

[91] I. Holme, "Innovative technologies for high performance textiles," *Color. Technol.*, vol. 123, pp. 59–73, 2007, doi: 10.1111/j.1478-4408.2007.00064.x.

[92] K. Shrimali and E. M. Dedhia, "Microencapsulation for Textile Finishing," *IOSR J. Polym. Text. Eng.*, vol. 2, no. 2, pp. 1–4, 2015, doi: 10.9790/019X-0220104.

[93] R. Cerbino, "Quantitative optical microscopy of colloids: The legacy of Jean Perrin," *Curr. Opin. Colloid Interface Sci.*, vol. 34, pp. 47–58, 2018, doi: 10.1016/j.cocis.2018.03.003.

[94] J. O. Fiedler, O. G. Carmona, C. G. Carmona, M. J. Lis, A. M. S. Plath, R. B. Samulewski, and F. M. Bezerra, "Application of Aloe vera microcapsules in cotton nonwovens to obtain biofunctional textiles," *J. Text. Inst.*, vol. 111, no. 1, pp. 68–74, 2020, doi: 10.1080/00405000.2019.1625607.

[95] R. H. Webb, "Confocal optical microscopy," *Rep. Prog. Phys.*, vol. 59, pp. 427–471, 1996.

[96] A. W. Coats and J. P. Redfern, "Thermogravimetric Analysis," *Analyst*, vol. 88, pp. 906–924, 1963.

[97] R. Xu, “Light scattering: A review of particle characterization applications,” *Particuology*, vol. 18, pp. 11–21, 2015, doi: 10.1016/j.partic.2014.05.002.

[98] A. George, P. A. Shah, and P. S. Shrivastav, “Natural biodegradable polymers based nano-formulations for drug delivery: A review,” *Int. J. Pharm.*, vol. 561, pp. 244–264, 2019, doi: 10.1016/j.ijpharm.2019.03.011.

[99] V. Ruseva, M. Lyons, J. Powell, J. Austin, A. Malm, and J. Corbett, “Capillary dynamic light scattering: Continuous hydrodynamic particle size from the nano to the micro-scale,” *Colloids Surfaces A Physicochem. Eng. Asp.*, vol. 558, pp. 504–511, 2018, doi: 10.1016/j.colsurfa.2018.09.022.

[100] S. F. Hosseini, M. Zandi, M. Rezaei, and F. Farahmandghavi, “Two-step method for encapsulation of oregano essential oil in chitosan nanoparticles: Preparation, characterization and in vitro release study,” *Carbohydr. Polym.*, vol. 95, pp. 50–56, 2013, doi: 10.1016/j.carbpol.2013.02.031.

[101] B. Liao and E. Najafi, “Scanning ultrafast electron microscopy: A novel technique to probe photocarrier dynamics with high spatial and temporal resolutions,” *Mater. Today Phys.*, vol. 2, pp. 46–53, 2017, doi: 10.1016/j.mtphys.2017.07.003.

[102] S. Westworth, N. Ashwath, and D. Cozzolino, “Application of FTIR-ATR spectrocopy to detect salinity response in Beauty leaf tree (calophyllum inophyllam L),” *Energy Procedia*, vol. 160, pp. 761–768, 2019, doi: 10.1016/j.egypro.2019.02.182.

[103] T. Petit and L. Puskar, “FTIR spectroscopy of nanodiamonds: Methods and interpretation,” *Diam. Relat. Mater.*, vol. 89, pp. 52–66, 2018, doi: 10.1016/j.diamond.2018.08.005.

[104] V. Rubentheren, T. A. Ward, C. Yern, and C. Kuang, “Processing and analysis of chitosan nanocomposites reinforced with chitin whiskers and tannic acid as a crosslinker,” *Carbohydr. Polym.*, vol. 115, pp. 379–387, 2015, doi: 10.1016/j.carbpol.2014.09.007.

[105] C. Butstraen and F. Salaün, “Preparation of microcapsules by complex coacervation of gum Arabic and chitosan,” *Carbohydr. Polym.*, vol. 99, pp. 608–616, 2014, doi: 10.1016/j.carbpol.2013.09.006.

[106] R. A. Clará, A. C. G. Marigliano, V. del V. Campos, and H. N. Sólimo, “Density, viscosity, vapour-liquid equilibrium, excess molar enthalpy, and their correlations of the binary system [1-pentanol + R-(+)-limonene] over the complete concentration range, at different temperatures,” *Fluid Phase Equilib.*, vol. 293, pp. 151–156, 2010, doi: 10.1016/j.fluid.2010.03.001.

[107] B. Muhoza, S. Xia, and X. Zhang, “Gelatin and high methyl pectin coacervates crosslinked with tannic acid: The characterization, rheological properties, and application for peppermint oil microencapsulation,” *Food Hydrocoll.*, vol. 97, p. 105174, 2019, doi: 10.1016/j.foodhyd.2019.105174.

[108] Z. Xiao, W. Liu, G. Zhu, R. Zhou, and Y. Niu, “Production and characterization of multinuclear microcapsules encapsulating lavender oil by complex coacervation,” *Flavour Fragr. J.*, vol. 29, pp. 166–172, 2014, doi: 10.1002/ffj.3192.

[109] I. Gülseren and M. Corredig, “Interactions at the interface between hydrophobic and hydrophilic emulsifiers: Polyglycerol polyricinoleate (PGPR) and milk proteins, studied by drop shape tensiometry,” *Food Hydrocoll.*, vol. 29, pp. 193–198, 2012, doi: 10.1016/j.foodhyd.2012.03.010.

[110] D. J. McClements and S. M. Jafari, “Improving emulsion formation, stability and performance using mixed emulsifiers: A review,” *Adv. Colloid Interface Sci.*, vol. 251, pp. 55–79, 2018, doi: 10.1016/j.cis.2017.12.001.

[111] R. Wilson, B. J. Van Schie, and D. Howes, “Overview of the Preparation, Use and Biological Studies on Polyglycerol Polyricinoleate (PGPR),” *Food Chem. Toxicol.*, vol. 36, pp. 711–718, 1998, doi: 10.1016/S0278-6915(98)00057-X.

[112] A. L. Márquez, A. Medrano, L. A. Panizzolo, and J. R. Wagner, “Effect of calcium salts and surfactant concentration on the stability of water-in-oil (w/o) emulsions prepared with polyglycerol polyricinoleate,” *J. Colloid Interface Sci.*, vol. 341, pp. 101–108, 2010, doi: 10.1016/j.jcis.2009.09.020.

[113] K. Kato, P. Walde, N. Koine, Y. Imai, K. Akiyama, and T. Sugahara, “Molecular Composition of Nonionic Vesicles Prepared from Span 80 or Span 85 by a Two-Step Emulsification Method,” *J. Dispers. Sci. Technol.*, vol. 27, pp. 1217–1222, 2006, doi: 10.1080/01932690600859903.

[114] R. Afshar Ghotli, A. A. A. Raman, S. Ibrahim, and S. Baroutian, “Liquid-Liquid Mixing in Stirred Vessels: a Review,” *Chem. Eng. Commun.*, vol. 200, pp. 595–627, 2013, doi: 10.1080/00986445.2012.717313.

[115] S. J. Park, Y. S. Shin, and J. R. Lee, “Preparation and Characterization of Microcapsules Containing Lemon Oil,” *J. Colloid Interface Sci.*, vol. 241, pp. 502–508, 2001, doi: 10.1006/jcis.2001.7727.

[116] M. A. Cremasco, *Operações unitárias em sistemas particulados e fluidomecânicos*, 3rd ed. São Paulo: Blucher, 2018.

[117] BIOVERA, “Agitador mecânico ou agitador de hélice.” https://www.biovera.com.br/noticias/agitador-mecanico-ou-agitador-de-helice/.

[118] C. Tan, J. Xie, X. Zhang, J. Cai, and S. Xia, “Polysaccharide-based nanoparticles by chitosan and gum arabic polyelectrolyte complexation as carriers for curcumin,” *Food Hydrocoll.*, vol. 57, pp. 236–245, 2016, doi: 10.1016/j.foodhyd.2016.01.021.

[119] G. P. Kumar and P. Rajeshwarrao, “Nonionic surfactant vesicular systems for effective drug delivery—an overview,” *Acta Pharm. Sin. B*, vol. 1, no. 4, pp. 208–219, 2011, doi: 10.1016/j.apsb.2011.09.002.

[120] P. Monllor, L. Capablanca, J. Gisbert, P. Díaz, I. Montava, and Á. Bonet, “Improvement of Microcapsule Adhesion to Fabrics,” *Text. Res. J.*, vol. 80, no. 7, pp. 631–635, 2010, doi: 10.1177/0040517509346444.

[121] D. V. Mendanha, S. E. Molina Ortiz, C. S. Favaro-Trindade, A. Mauri, E. S. Monterrey-Quintero, and M. Thomazini, “Microencapsulation of casein hydrolysate by complex coacervation with SPI/pectin,” *Food Res. Int.*, vol. 42, pp. 1099–1104, 2009, doi: 10.1016/j.foodres.2009.05.007.

[122] C. Dima, M. Cotârlet, P. Alexe, and S. Dima, “Microencapsulation of essential oil of pimento [Pimenta dioica (L) Merr.] by chitosan/k-carrageenan complex coacervation method,” *Innov. Food Sci. Emerg. Technol.*, vol. 22, pp. 203–211, 2014, doi: 10.1016/j.ifset.2013.12.020.

Appendix

Appendix A – Optical Microscopy.

Table A.1 - Optical microscopy analysis at different stages of the microcapsule production process.

Assays	Sample after emulsification (200× or 400× magnification)	Sample at 40 °C in the reactor (400× magnification)	Sample at 5 °C in the reactor (200× or 400× magnification)	Sample after synthesis in the reactor (200× or 400× magnification)	Final sample of microcapsules (400× magnification)
1	*none*	*none*	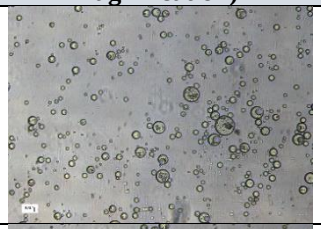	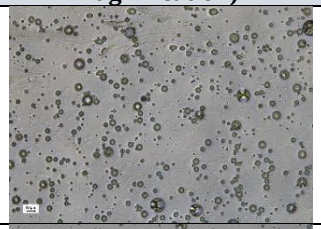	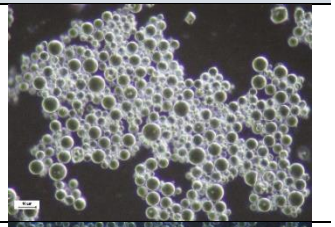
2	*none*	*none*	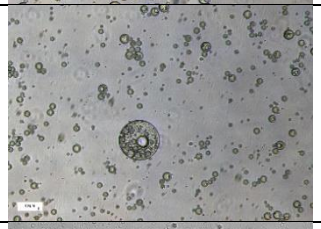	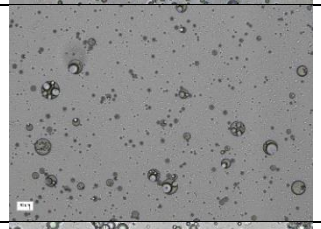	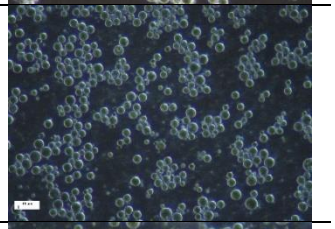
3	*none*	*none*		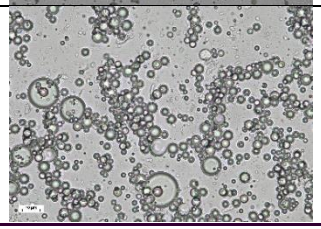	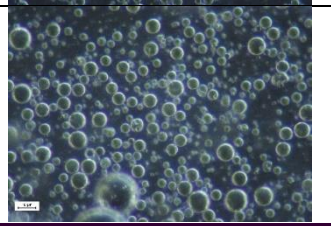

4	*none*	*none*	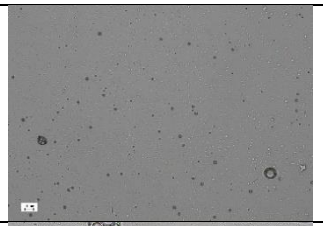	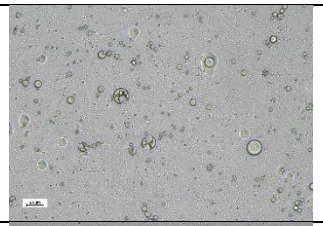	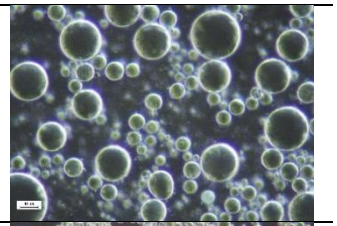
5	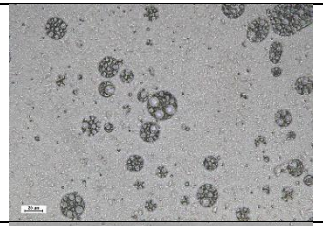				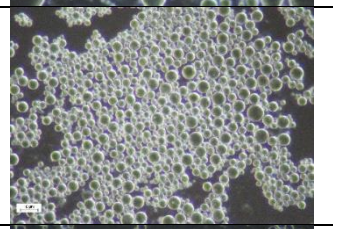
6	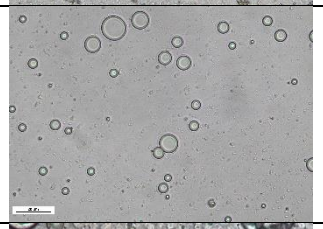		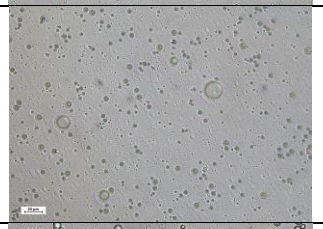	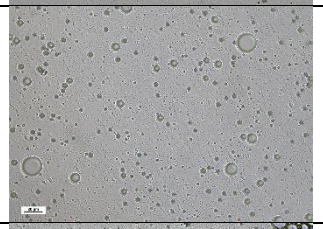	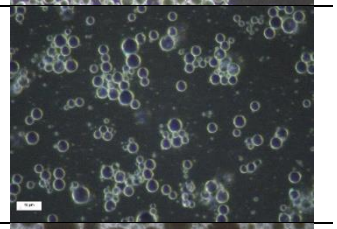
7	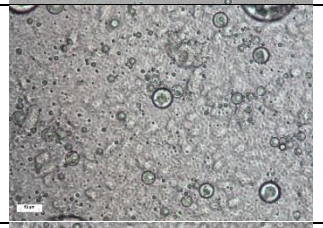	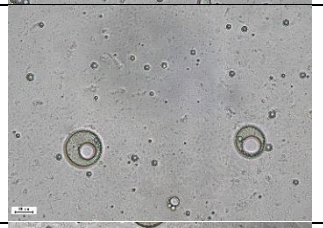			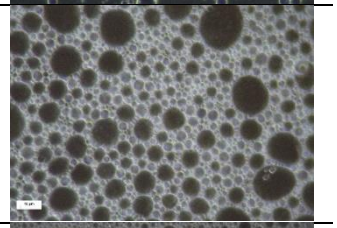
8	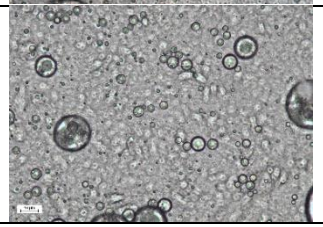			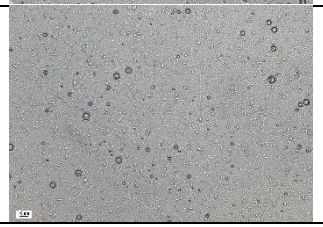	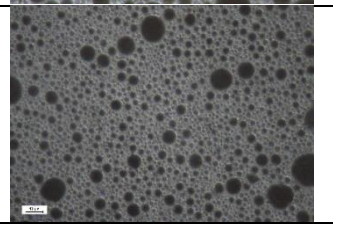

9	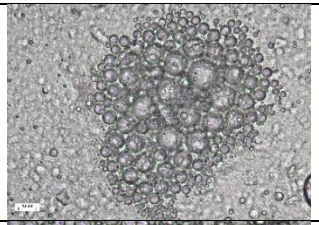	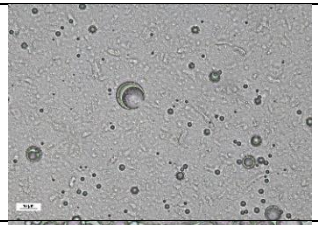		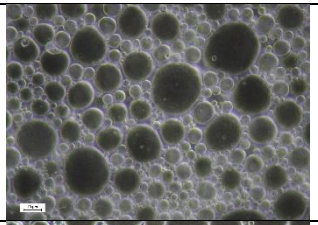	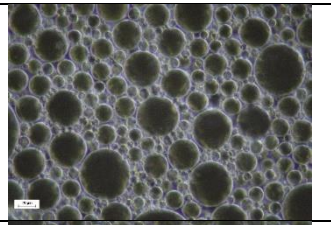
10	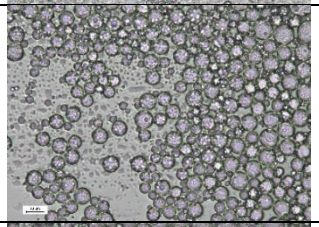	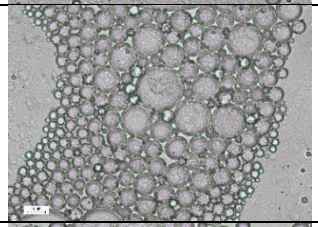	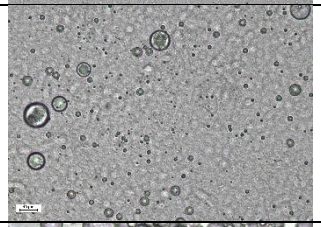	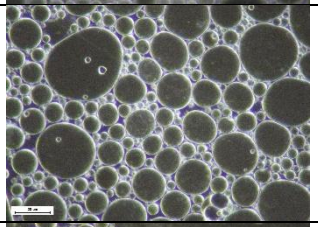	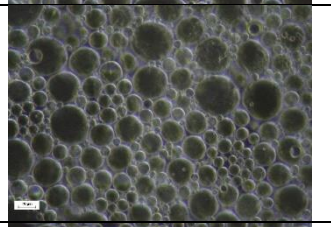
11	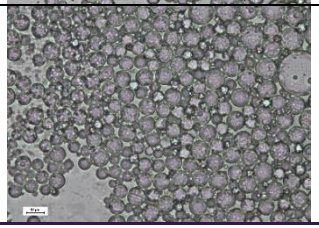	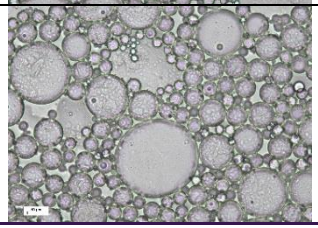	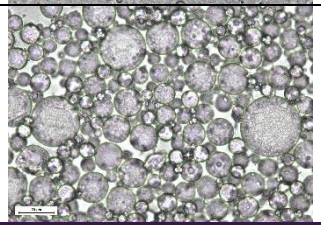	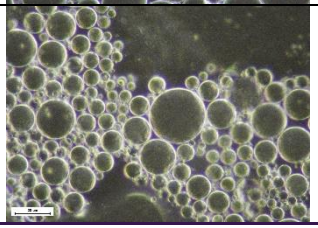	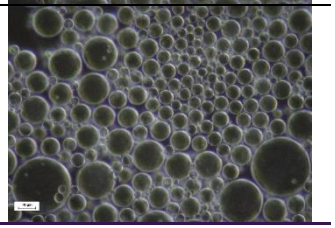

Table A.2 - Optical microscopy of the lower phase of the decantation funnel of assays 8 to 11, after initial decantation, after the first wash with water and after the second wash with water.

Assays	Sample after initial decantation (magnification 400×)	Sample after first wash (magnification 400×)	Sample after second wash (magnification 400×)
8	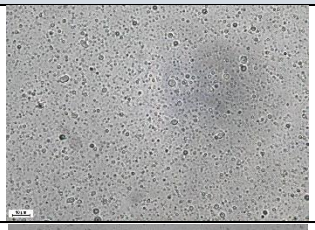	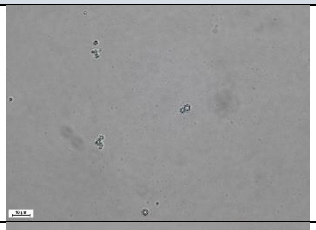	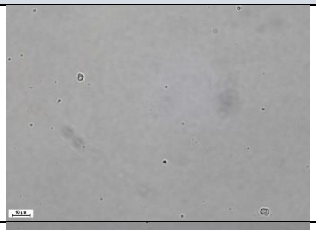
9	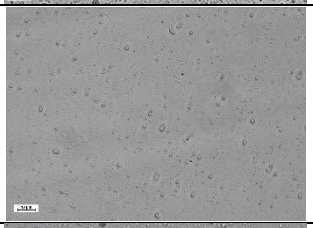		
10		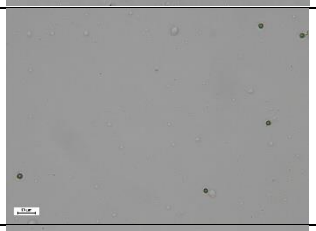	
11	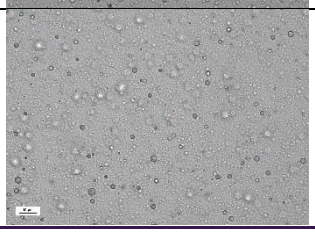	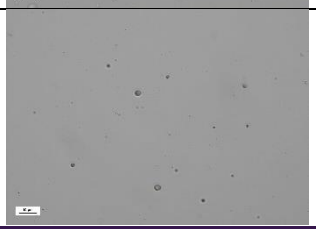	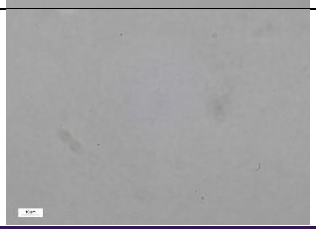

Appendix B – Particle Size Evaluation.

Table B.1 - Detailed data of the particle size evaluation in volume of the microcapsules produced in the assays from 8 to 11.

Assays	D10 (µm)	St. Dev. (µm)	D50 (µm)	St. Dev. (µm)	D90 (µm)	St. Dev. (µm)	Laser obscuration (%)	St. Dev. (%)
Before the washing step								
8	1.08	± 0.0050	1.94	± 0.0120	4.11	± 0.0490	5.80	± 0.240
9	1.22	± 0.0031	2.36	± 0.0058	8.35	± 0.3700	4.67	± 0.240
10	1.03	± 0.0009	2.14	± 0.0027	47.10	± 0.5500	5.03	± 0.140
10 Triton™	*	*	*	*	*	*	*	*
11	1.00	± 0.0006	2.03	± 0.0043	58.70	± 1.1200	5.50	± 0.060
After the washing step								
8	1.10	± 0.0020	137.00	± 0.5260	263.00	± 2.4900	3.97	± 0.100
9	1.01	± 0.0014	2.25	± 0.0109	75.50	± 0.4030	5.56	± 0.110
10	1.06	± 0.0043	2.42	± 0.0267	64.10	± 1.1200	5.41	± 0.410
10 Triton™	0.95	± 0.0021	1.92	± 0.0011	51.00	± 0.7230	5.72	± 0.240
11	0.97	± 0.0062	2.12	± 0.0072	96.60	± 1.9300	4.16	± 0.320

* Regarding data from assay 10

Table B.2 – Detailed data of the particle size evaluation in number of the microcapsules produced in the assays from 8 to 11.

Assays	D10 (µm)	St. Dev. (µm)	D50 (µm)	St. Dev. (µm)	D90 (µm)	St. Dev. (µm)	Laser obscuration (%)	St. Dev. (%)
Before the washing step								
8	0.77	± 0.0020	1.12	± 0.0040	1.87	± 0.0080	5.80	± 0.240
9	0.84	± 0.0018	1.22	± 0.0028	2.07	± 0.0044	4.67	± 0.240
10	0.69	± 0.0005	1.00	± 0.0009	1.66	± 0.0028	5.03	± 0.140
10 Triton™	*	*	*	*	*	*	*	*
11	0.67	± 0.0001	0.97	± 0.0001	1.62	± 0.0002	5.50	± 0.060
After the washing step								
8	0.51	± 0.0030	0.74	± 0.0040	1.20	± 0.0080	3.97	± 0.100
9	0.66	± 0.0018	0.96	± 0.0025	1.59	± 0.0047	5.56	± 0.110
10	0.69	± 0.0045	1.01	± 0.0077	1.67	± 0.0172	5.41	± 0.410
10 Triton™	0.65	± 0.0016	0.94	± 0.0026	1.55	± 0.0050	5.72	± 0.240
11	0.64	± 0.0050	0.93	± 0.0074	1.54	± 0.0142	4.16	± 0.320

* Regarding data from assay 10